

The Geography of Recent Genetic Ancestry across Europe.

Peter Ralph¹ and Graham Coop¹

¹ Department of Evolution and Ecology & Center for Population Biology,

University of California, Davis.

To whom correspondence should be addressed: plralph@ucdavis.edu, gcoop@ucdavis.edu

Abstract

The recent genealogical history of human populations is a complex mosaic formed by individual migration, large-scale population movements, and other demographic events. Population genomics datasets can provide a window into this recent history, as rare traces of recent shared genetic ancestry are detectable due to long segments of shared genomic material. We make use of genomic data for 2,257 Europeans (the POPRES dataset) to conduct one of the first surveys of recent genealogical ancestry over the past three thousand years at a continental scale. We detected 1.9 million shared genomic segments, and used the lengths of these to infer the distribution of shared ancestors across time and geography. We find that a pair of modern Europeans living in neighboring populations share around 10–50 genetic common ancestors from the last 1500 years, and upwards of 500 genetic ancestors from the previous 1000 years. These numbers drop off exponentially with geographic distance, but since genetic ancestry is rare, individuals from opposite ends of Europe are still expected to share millions of common genealogical ancestors over the last 1000 years. There is substantial regional variation in the number of shared genetic ancestors: especially high numbers of common ancestors between many eastern populations likely date to the Slavic and/or Hunnic expansions, while much lower levels of common ancestry in the Italian and Iberian peninsulas may indicate weaker demographic effects of Germanic expansions into these areas and/or more stably structured populations. Recent shared ancestry in modern Europeans is ubiquitous, and clearly shows the impact of both small-scale migration and large historical events. Population genomic datasets have considerable power to uncover recent demographic history, and will allow a much fuller picture of the close genealogical kinship of individuals across the world.

Author Summary

Few of us know our family histories more than a few generations back. Therefore, it is easy to overlook the fact that we are all distant cousins, related to one another via a vast network of relationships. Here we use genome-wide data from European individuals to investigate these relationships over the past three thousand years, by looking for long stretches of shared genome between pairs of individuals inherited from common genetic ancestors. We quantify this ubiquitous recent common ancestry, showing that for instance even pairs of individuals on opposite sites of Europe share hundreds of genetic common ancestors over this time period. Despite this degree of commonality, there are also striking regional differences. For instance, southeastern Europeans share large numbers of common ancestors which date to the era of the Slavic and Hunnic expansions around 1,500 years ago, while most common ancestors that Italians share with other populations lived longer ago than 2,500 years. The study of long stretches of shared genetic material holds the promise of rich information about many aspects of recent population history.

1 Introduction

Even seemingly unrelated humans are distant cousins to each other, as all members of a species are related to each other through a vastly ramified family tree (their pedigree). We can see traces of these relationships in genetic data when individuals inherit shared genetic material from a common ancestor. Traditionally, population genetics has studied the distant bulk of these genetic relationships, which in humans typically date from hundreds of thousands of years ago (e.g. Cann et al., 1987; Takahata, 1993). Such studies have provided deep insights into the origins of modern humans (e.g. Li and Durbin, 2011), and into recent admixture between diverged populations (e.g. Moorjani et al., 2011; Henn et al., 2012a).

Although most such genetic relationships among individuals are very old, some individuals are related on far shorter time scales. Indeed, given that each individual has 2^n ancestors from n generations ago, theoretical considerations suggest that all humans are related genealogically to each other over surprisingly short time scales (Chang, 1999; Rohde et al., 2004). We are usually unaware of these close genealogical ties, as few of us have knowledge of family histories more than a few generations back, and these ancestors often do not contribute genetic material to us (Donnelly, 1983). However, in large samples we can hope to identify genetic evidence of more recent relatedness, and so obtain insight into the population history of the past tens of generations. Here we investigate patterns of recent relatedness in a large European dataset.

The past several thousand years are replete with events that may have had significant impact on modern European relatedness, from the Neolithic expansion of farming to the Roman empire and the much more recent expansions of the Slavs and the Vikings. Our current understanding of these events is deduced from archaeological, linguistic, cultural, historical, and genetic evidence, with widely varying degrees of certainty. However, the demographic and genealogical impact of these events is still uncertain, with some theories holding that group identity was fluid to the point that such groups would have maintained very little coherence in terms of ancestry (Gillett, 2006). Genetic data describing the breadth of genealogical relationships, can therefore add another dimension to our understanding of these historical events.

Work from uniparentally inherited markers (mtDNA and Y chromosomes) has improved our understanding of human demographic history (e.g. Soares et al., 2010). However, interpretation of these markers is difficult since they only record a single lineage of each individual (the maternal and paternal lineages, respectively), rather than the entire distribution of ancestors. Genome-wide genotyping and sequencing datasets have the potential to provide a much richer picture of human history, as we can learn simultaneously about the diversity of ancestors that contributed to each individual’s genome.

A number of studies have begun to reveal quantitative insights into recent human history (Novembre and Ramachandran, 2011). Within Europe, the first two principal axes of variation of the matrix of genotypes are closely related to a rotation of latitude and longitude (Menozzi et al., 1978; Novembre et al., 2008; Lao et al., 2008), as would be expected if patterns of ancestry are mostly shaped by local migration (Novembre and Stephens, 2008). Other work has revealed a slight decrease in diversity running from south-to-north in Europe, with the highest haplotype and allelic diversity in the Iberian peninsula (e.g. Auton et al., 2009; Nelson et al., 2012), and the lowest haplotype diversity in England and Ireland (O’Dushlaine et al., 2010). However, we currently have little sense of the time scale of the historical events underlying these geographic patterns, nor the degrees of genealogical relatedness they imply.

In this paper, we analyze those rare long chunks of genome that are shared between pairs of individuals due to inheritance from recent common ancestors, to obtain a detailed view of the geographic structure of recent relatedness. To determine the time scale of these relationships, we develop methodology that uses the lengths of shared genomic segments to infer the distribution of the ages of these recent common ancestors. We find that even geographically distant Europeans share ubiquitous common ancestry even within the past 1,000 years, and show that common ancestry from the past 3,000 years is a result of both local migration and large-scale historical events.

1.1 Definitions: Genetic ancestry and identity by descent

Genetic data can only hope to inform us about those ancestors from whom a pair of individuals have both inherited a common genomic region, in which case the ancestor is a “genetic common ancestor”,

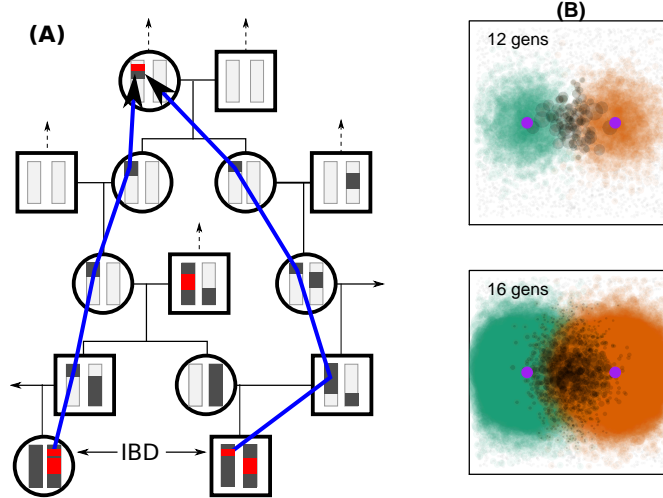


Figure 1: **(A)** A hypothetical portion of the pedigree relating two sampled individuals, which shows six of their shared genealogical common ancestors, with the portions of ancestral chromosomes from which the sampled individuals have inherited shaded grey. The IBD blocks they have inherited from the two genetic common ancestors are colored red, and the blue arrow denotes the path through the pedigree along which one of these IBD blocks was inherited. **(B)** Cartoon of the spatial locations of ancestors of two individuals – circle size is proportional to likelihood of genetic contribution, and shared ancestors are marked in grey. Note that common ancestors are likely located between the two, and their distribution becomes more diffuse further back in time.

and the region is shared “identical by descent” (IBD) by the two. We define an “IBD block” to be a contiguous segment of genome inherited (on at least one chromosome) from a shared common ancestor without intervening recombination (see figure 1A). Historically, a more usual definition of IBD restricts to those segments inherited from some prespecified set of “founder” individuals (e.g. Fisher, 1954; Donnelly, 1983; Chapman and Thompson, 2002). We differ because we allow ancestors to be arbitrarily far back in time. Under our definition, everyone is IBD everywhere, but mostly on very short, old segments (Powell et al., 2010). We measure lengths of IBD segments in units of Morgans (M) or centiMorgans (cM), where 1 Morgan is defined to be the distance over which an average of one recombination (i.e. a crossover) occurs per meiosis. Segments of IBD are broken up over time by recombination, which implies that older shared ancestry tends to result in shorter shared IBD blocks.

Sufficiently long segments of IBD can be identified as long, contiguous regions over which the two individuals are identical (or nearly identical) at a set of Single Nucleotide Polymorphisms (SNPs) which segregate in the population. Formal, model-based methods to infer IBD are only computationally feasible for very recent ancestry (e.g. Brown et al., 2012), but recently, fast heuristic algorithms have been developed that can be applied to thousands of samples typed on genotyping chips (e.g. Browning and Browning, 2011; Gusev et al., 2009).

The relationship between numbers of long, shared segments of genome, numbers of genetic common ancestors, and numbers of genealogical common ancestors can be difficult to envision. Since everyone has exactly two biological parents, every individual has exactly 2^n paths of length n leading back through their pedigree, each such path ending in a grand $^{n-1}$ parent. However, due to Mendelian segregation and limited recombination, genetic material will only be passed down along a small subset of these paths (Donnelly, 1983). As n grows, these paths proliferate rapidly and so the genealogical paths of two individuals soon overlap significantly. (These points are illustrated in in figure 1.) By observing the number of shared genomic blocks, we learn about the number of paths through the pedigree along which both individuals have

inherited genetic material.

At least one parent of each genetic common ancestor of two individuals is also a genetic common ancestor, but the relevant quantity is the time back to the most recent such common genetic ancestor. For this reason, when we say “genetic common ancestor” or “rate of genetic common ancestry”, we are referring to only the *most recent* genetic common ancestors from which the individuals in question inherited their shared segments of genome. This quantity can also be more intuitive – for instance, a randomly mating population of constant size will have a constant rate of appearance of most recent genetic common ancestors (the coalescent rate, Hudson, 1990). The total number of unqualified genetic common ancestors is lower bounded by the total number of most recent genetic common ancestors that have so far appeared; and since we deal with fairly small numbers of generations and fairly short pieces of genome, the true number of genetic ancestors only differs by a small factor.

2 Results

We applied the `fastIBD` method (with some modifications), implemented in `BEAGLE` (Browning and Browning, 2011), to the POPRES dataset (Nelson et al., 2008), which includes language and country-of-origin data for several thousand Europeans genotyped at 500,000 SNPs. Our simulations showed that we have good power to detect long IBD blocks (probability of detection 50% for blocks longer than 2cM, rising to 98% for blocks longer than 4cM), and a low false positive rate (see figure 6 below). We restricted our analysis to individuals who reported all grandparents from the same European country (so this is who we refer to as “Europeans”). After removing obvious outlier individuals and close relatives, we were left with 2,257 individuals which we grouped using reported country of origin and language into 40 populations, listed with sample sizes and average IBD levels in table 1. For geographic analyses, we located each population at the largest population city in the appropriate region. Pairs of individuals in this dataset were found to share a total of 1.9 million segments of IBD, an average of 0.74 per pair of individuals, or 831 per individual. The mean length of these blocks was 2.5cM, the median was 2.1cM and the 25th and 75th quantiles are 1.5cM and 2.9cM respectively. The majority of pairs sharing IBD shared only a single block of IBD (94%). Between 30% and 250% of The genome of each individual is covered by blocks of IBD.

The observed genomic density of long IBD blocks (per cM) can be affected by recent selection (Albrechtsen et al., 2010) and by recombination modifiers. We find that the local density of IBD blocks of all lengths is relatively constant across the genome, but in certain regions the length distribution is systematically perturbed (see supplemental figure S1), including around certain centromeres and the large inversion on chromosome 8 (Giglio et al., 2001), also seen by Albrechtsen et al. (2010). Somewhat surprisingly, the MHC does not show an unusual pattern of IBD, despite having shown up in other genomic scans for IBD (Albrechtsen et al., 2010; Gusev et al., 2012). However, there are a few other regions where differences in IBD rate are not predicted by differences in SNP density. Notably, there are two regions, on chromosomes 15 and 16, which are nearly as extreme in their deviations in IBD as the inversion on chromosome 8, and may also correspond to large inversions segregating in the sample. These only make up a small portion of the genome, and do not significantly affect our other analyses; we leave further analysis for future work.

2.1 Substructure and recent migrants

We should expect significant within-population variability, as modern countries are relatively recent constructions of diverse assemblages of languages and heritages. To assess the uniformity of ancestry within populations, we used a permutation test to measure, for each pair of populations x and y , the uniformity with which relationships with x are distributed across individuals from y . Most comparisons show statistically significant substructure (supplemental figure S2). A notable exception is that nearly all populations showed no significant partitioning of numbers of common ancestors with Italian samples, suggesting that most common ancestors shared with Italy lived longer ago than the time that structure within modern-day countries formed.

E group						N group					
		<i>n</i>	self	other				<i>n</i>	self	other	
Czech Republic	Albania	AL	9	14.5	1.7	Denmark	DK	1	–	0.9	
	Austria	AT	14	1.3	0.9	Finland	FI	1	–	1.2	
	Bosnia	BO	9	4.1	1.6	Latvia	LV	1	–	1.6	
	Bulgaria	BG	1	–	1.3	Norway	NO	2	2.0	0.8	
	Croatia	HR	9	2.8	1.6	Sweden	SE	10	3.4	1.0	
	Czech Republic	CZ	9	2.1	1.3						
	Greece	EL	5	1.8	0.9	W group					
	Hungary	HU	19	1.9	1.2	Belgium	BE	37	1.1	0.6	
	Kosovo	KO	15	9.9	1.7	England	EN	22	1.3	0.7	
	Montenegro	ME	1	–	1.8	France	FR	86	0.7	0.5	
	Macedonia	MA	4	2.5	1.4	Germany	DE	71	1.1	0.9	
	Poland	PL	22	3.8	1.5	Ireland	IE	60	2.6	0.6	
	Romania	RO	14	2.1	1.2	Netherlands	NL	17	1.9	0.7	
	Russia	RU	6	4.3	1.4	Scotland	SC	5	2.2	0.7	
	Slovenia	SI	2	5.0	1.3	Swiss French	CHf	839	1.3	0.6	
	Serbia	RS	11	2.7	1.5	Swiss German	CHd	103	1.6	0.6	
Slovakia	SK	1	–	0.7	Switzerland	CH	17	1.1	0.5		
Ukraine	UA	1	–	1.5	United Kingdom	UK	358	1.2	0.7		
Yugoslavia	YU	10	3.4	1.5							
TC group						I group					
		<i>n</i>	self	other				<i>n</i>	self	other	
	Cyprus	CY	3	2.7	0.4	Italy	IT	213	0.6	0.5	
	Turkey	TR	4	2.2	0.5	Portugal	PT	115	1.9	0.5	
						Spain	ES	130	1.5	0.4	

Table 1: Populations, abbreviations, sample sizes (n), mean number of IBD blocks shared by a pair of individuals from that population (“self”), and mean IBD rate averaged across all other populations (“other”); sorted by regional groupings described in the text. Populations with only a single sample do not have a “self” IBD rate.

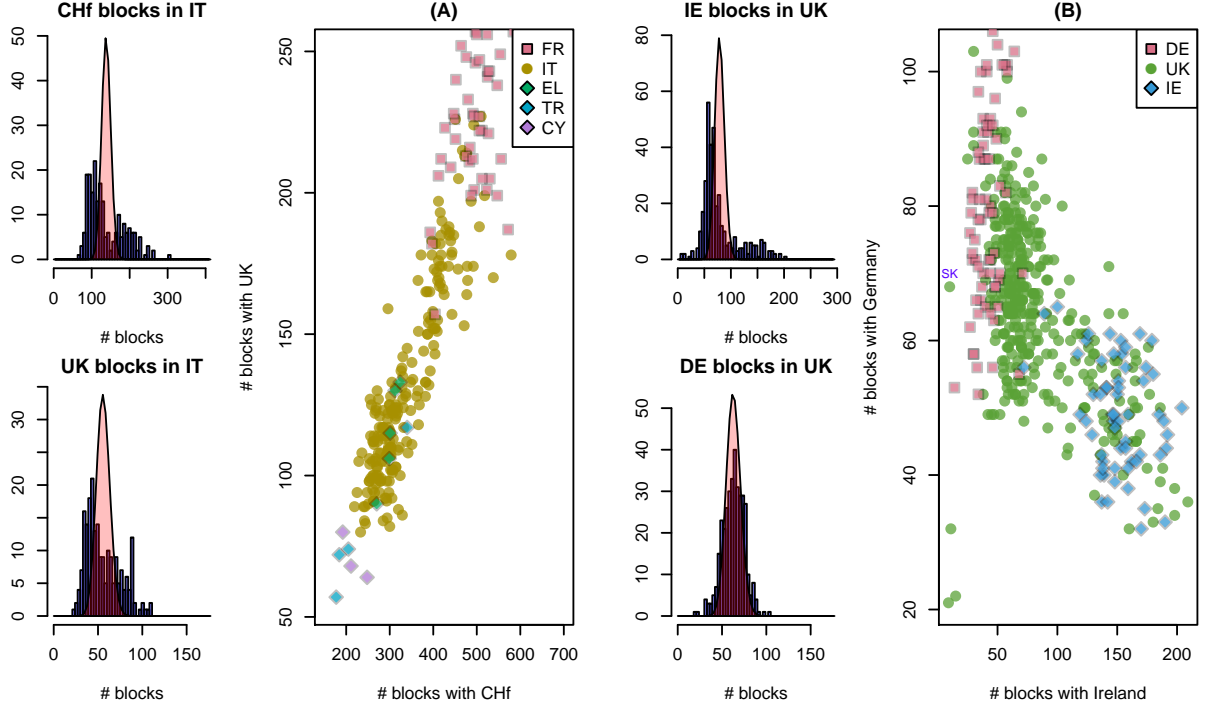


Figure 2: Substructure, in **(A)** Italian, and **(B)** UK samples. The leftmost plots of **(A)** show histograms of the numbers of IBD blocks that each Italian sample shares with any French-speaking Swiss (top) and anyone from the UK (bottom), overlaid with the expected distribution (Poisson) if there was no substructure. Next is shown a scatterplot of numbers of blocks shared with French-speaking Swiss and UK samples, for all samples from France, Italy, Greece, Turkey, and Cyprus. We see that the numbers of recent ancestors each Italian shares with the French-speaking Swiss and with the United Kingdom are both bimodal, and that these two are positively correlated, ranging continuously between values typical for Turkey/Cyprus and for France. Figure **(B)** is similar, showing that the substructure within the UK is part of a continuous trend ranging from Germany to Ireland. The outliers visible in the scatterplot of figure 2B are easily explained as individuals with immigrant recent ancestors – the UK individuals in the lower left have many more Italian blocks than all other UK samples, and the individual labeled “SK” is a clear outlier for the number of blocks shared with the Slovakian sample.

Two of the more striking examples of substructure are illustrated in figure 2. Here, we see that variation within countries can be reflective of continuous variation in ancestry that spans a broader geographic region, crossing geographic, political and linguistic boundaries. Figure 2A shows the distinctly bimodal distribution of numbers of IBD blocks that each Italian shares with both French-speaking Swiss and the UK, and that these numbers are strongly correlated. Furthermore, the amount that Italians share with these two populations varies continuously from values typical for Turkey and Cyprus, to values typical for France and Switzerland. Interestingly, the Greek samples (EL) place near the middle of the Italian gradient. It is natural to guess that there is a north-south gradient of recency of common ancestry along the length of Italy, and that southern Italy has been historically more closely connected to the eastern Mediterranean.

In contrast, within samples from the UK and nearby regions we see negative correlation between numbers of blocks shared with Irish and numbers of blocks shared with Germans. From our data, we do not know if this substructure is also geographically arranged within the UK. However, an obvious explanation of this pattern is that individuals within the UK differ in the extent of their recent Irish ancestry, and that individuals with less Irish ancestry have a larger portion of their recent ancestry shared with Germans. This suggests that there is variation across the UK – perhaps a geographic gradient – in terms of the amount of Celtic versus Germanic ancestry.

2.2 Europe-wide patterns of relatedness

Individuals usually share the highest number of IBD blocks with others from the same population, but with some exceptions. For example, individuals in the UK share more IBD blocks on average, and hence more close genetic ancestors, with individuals from Ireland than with other individuals from the UK, and Germans share similarly more with Polish than with other Germans. In figure 3 we depict the geography of rates of IBD sharing between populations, i.e. the average number of IBD blocks shared by a randomly chosen pair of individuals. Above, maps show the IBD rate relative to certain chosen populations (maps, above), and below, all pairwise sharing rates are plotted against the geographic distance separating the populations. It is evident that geographic proximity is a major determinant of IBD sharing (and hence recent relatedness), with the rate of pairwise IBD decreasing relatively smoothly as the geographic separation of the pair of populations increases.

Superimposed on this geographic decay there is striking regional variation in rates of IBD. To further explore this variation, we divided the populations into the four groups listed in table 1, using geographic location and correlations in the pattern of IBD sharing with other populations (shown in supplemental figure S4). These groupings are defined as: Europe “E”, lying to the east of Germany and Austria; Europe “N”, lying to the north of Germany and Poland; Europe “W”, to the west of Germany and Austria and including these; the Iberian and Italian peninsulas “I”; and Turkey/Cyprus “TC”. Although the general pattern of regional IBD variation is strong, none of these groups have sharp boundaries – for instance, Germany, Austria, and Slovakia are intermediate between E and W. Furthermore, we suspect that the Italian and Iberian peninsulas likely do not group together because of shared ancestry, but rather because of similarly low rates of IBD with other European populations. The overall mean IBD rates between these regions are shown in table 2, and comparisons between different groupings are colored differently in figure 3G–I, showing that rates of IBD sharing between E populations and between N populations average a factor of about three higher than other comparisons at similar distances.

To better understand IBD within these groupings, we show in figures 3G–I how average numbers of IBD blocks shared, in three different length categories, depend on the geographic distance separating the two populations. Even without taking into account regional variation, mean numbers of shared IBD blocks decay roughly exponentially with distance, and further structure is revealed by breaking out populations by regional groupings described above. The exponential decays shown for each pair of groupings emphasize how the decay of IBD with distance becomes more rapid for longer blocks. This is expected under models where migration is mostly local, since as one looks further back in time, the distribution of each individual’s ancestors is less concentrated around the individual’s location (recall figure 1B). Therefore, the expected number of ancestors shared by a pair of individuals decreases as the geographic distance between the pair increases; and rate of this decrease is larger for more recent ancestry.

This can also explain why the decay of IBD with distance varies significantly by region. For instance, the gradual decay of sharing with the Iberian and Italian peninsulas could occur because these blocks are inherited from much longer ago than blocks of similar lengths shared by individuals in other populations.

Conversely, the decay with distance is also quite gradual for “E–E” relationships. This is especially true for our shortest (oldest) blocks, where we see almost no decay with distance: individuals in our E grouping share on average almost as many short blocks with individuals in distant E populations as they do with others their own population. We argue below that this is because modern individuals in these locations have a larger proportion of their ancestors in a relatively small population that subsequently expanded.

IBD rate	E	I	N	TC	W
E	2.57	0.44	0.99	0.62	0.53
I	0.44	0.80	0.43	0.41	0.45
N	0.99	0.43	2.62	0.33	0.86
TC	0.62	0.41	0.33	1.43	0.25
W	0.53	0.45	0.86	0.25	0.93

Table 2: Rates of IBD within and between each geographic grouping given in table 1.

2.3 Timing and numbers of common ancestors

Each block of genome shared IBD represents genetic material inherited from a single genetic common ancestor shared by a pair of individuals – at least, the vast majority do, as these blocks come from long enough ago that it is highly unlikely for more than one block to be inherited along precisely the same path through the pedigree. Since the distribution of lengths of IBD blocks differs depending on the age of the ancestors – e.g. older blocks tend to be shorter – it is possible to use the distribution of lengths of IBD blocks to infer numbers of most recent genetic common ancestors back through time. This method is conceptually similar to the work of Pool and Nielsen (2009) and Gravel (2012), who used the length distribution of admixture tracts to infer parameters in demographic models.

Nature of the results on age inference There are two major difficulties to overcome, however. First, detection is noisy: we do not detect all IBD segments (especially shorter ones), and some of our IBD segments are false positives. This problem can be overcome by careful estimation and modeling of error, described in section 4.3. The second problem is more serious and unavoidable: as described in section 4.7, this inference problem is extremely “ill conditioned” (in the sense of Petrov and Sizikov, 2005), meaning in this case that there are many possible histories of shared ancestry that fit the data nearly equally well. For this reason, our results *necessarily* have a high degree of uncertainty, but still provide a good deal of useful information.

We deal with this uncertainty by describing the set of histories (i.e. historical numbers of common genetic ancestors) that are consistent with the data, summarized in two ways. First, it is useful to look at individual consistent histories, which gives a sense of recurrent patterns and possible historical signals. Figure 4 shows for several populations both the best-fitting history (in black) and the smoothest history that still fits the data (in red). We can make general statements if they hold across all (or most) consistent histories. Second, we can summarize the entire set of consistent histories by finding confidence intervals (bounds) for the total number of common ancestors aggregated in certain time periods. These are shown in Figure 5, giving estimates (colored bands) and bounds (vertical lines) for the total numbers of genetic common ancestors in each of three time periods, roughly 0–500ya, 500–1500ya, and 1500–2500ya (“ya” denotes “years ago”). Supplemental figure S5 is a version of figure 5 with more populations, and plots analogous to figure 4 for all these histories are shown in supplemental figure S7. For a precise description of the problem and our methods, see section 4.7.

The time periods we use for these bounds are quite large, but this is unavoidable, because of a trade off between temporal resolution and uncertainty in numbers of common ancestors. Also note that the lower

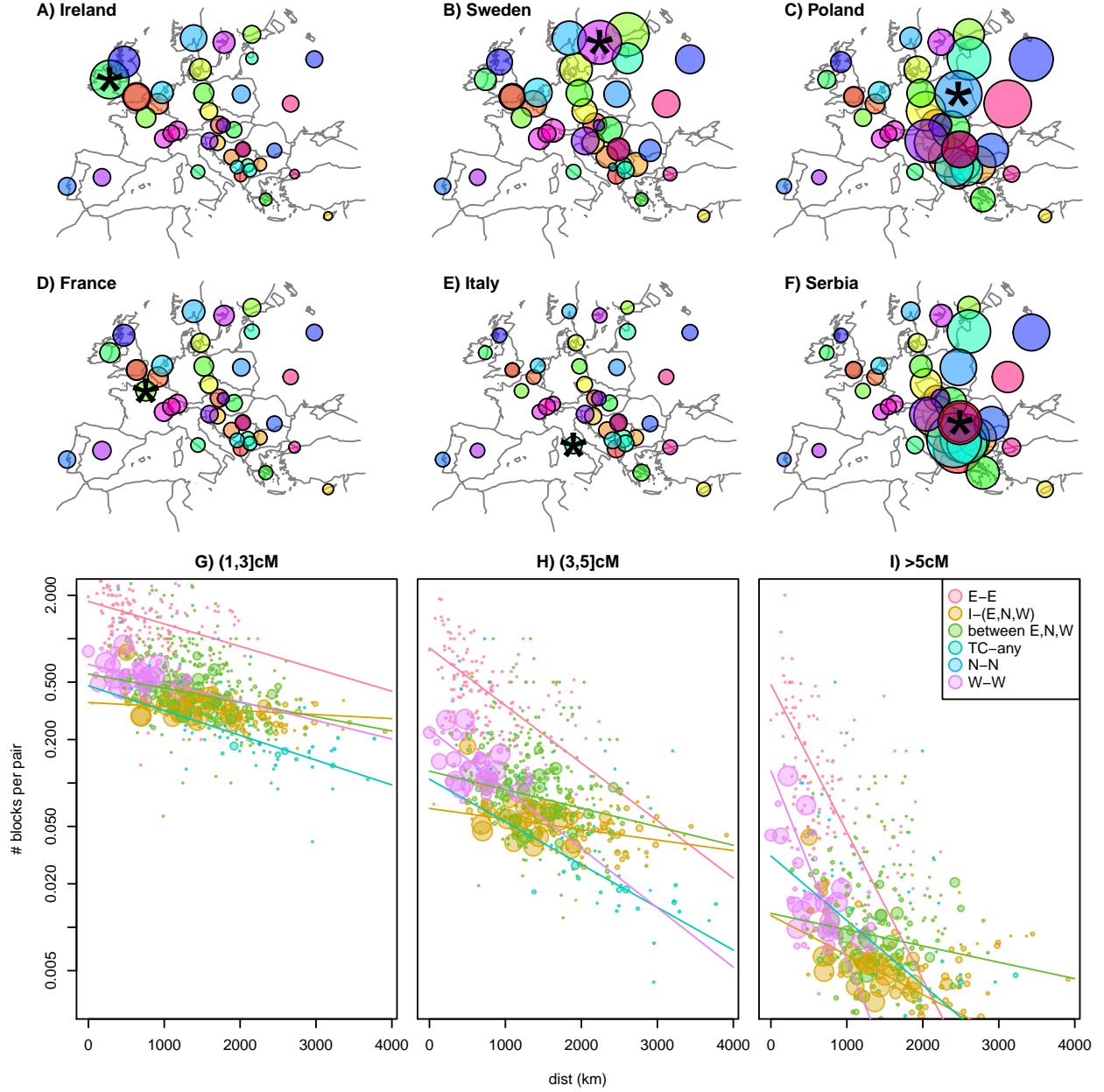


Figure 3: **(A–F)** The area of the circle area located on a particular population is proportional to the mean number of IBD blocks of length at least 1cM shared between random individuals chosen from that population and the population named in the label (also marked with a star). Both regional variation of overall IBD rates and gradual geographic decay are apparent. **(G–I)** Mean number of IBD blocks of lengths 1–3cM, 3–5cM, and >5cM, respectively, shared by a pair of individuals across all pairs of populations; the area of the point is proportional to sample size (number of distinct pairs), capped at a reasonable value. Colors give categories based on the regional groupings of table 1; and lines show an exponential decay fit to each category (using a Poisson GLM weighted by sample size). Comparisons with no shared IBD are used in the fit but not shown in the figure (due to the log scale). “E–E”, “N–N”, and “W–W” denote any two populations both in the E, N, or W grouping, respectively; “TC-any” denotes any population paired with Turkey or Cyprus; “I-(E,N,W)” denotes Italy paired with any population except Turkey or Cyprus; and “between E,N,W” denotes the remaining pairs (when both populations are in E, N, or W, but the two are in different groups). The exponential fit for the N–N points is not shown due to the very small sample size.

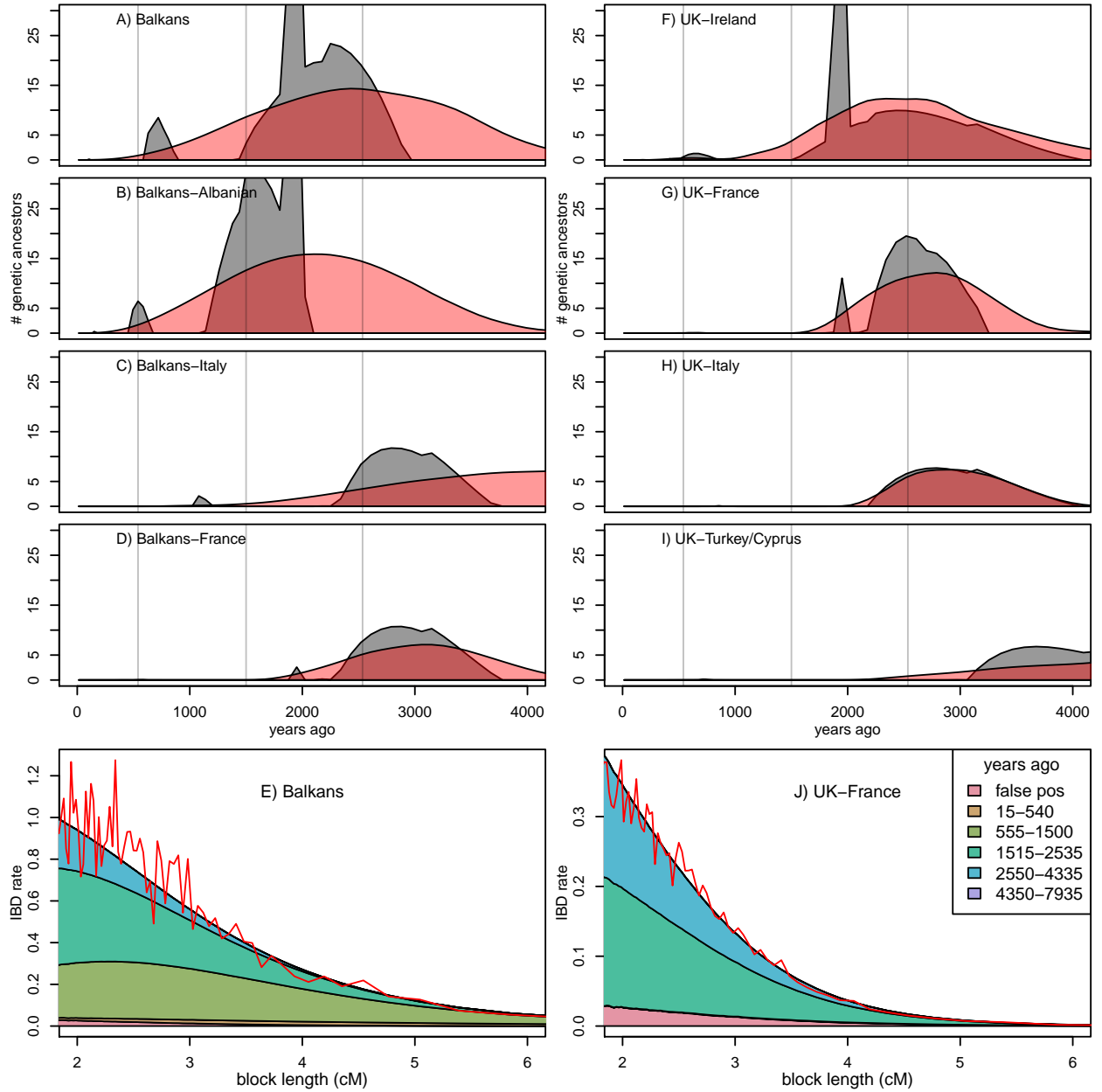


Figure 4: Estimated average number of genetic common ancestors per generation back through time shared by **(A)** pairs of individuals from “the Balkans” (former Yugoslavia, Bulgaria, Romania, Croatia, Bosnia, Montenegro, Macedonia, Serbia, and Slovenia, excluding Albanian speakers); and, shared by one individual from the Balkans with one individual from **(B)** Albanian speaking populations; **(C)** Italy; or **(D)** France. The black distribution is the maximum likelihood fit; shown in red is smoothest solution that still fits the data, as described in section 4.7. **(E)** shows the observed IBD length distribution for pairs of individuals from the Balkans (red curve), along with the distribution predicted by the smooth (red) distribution in the first figure, partitioned by time period in which the common ancestor lived. The second column of figures is similar, except that comparisons are relative to samples from the UK.

bounds on numbers of common ancestors during each time interval are often effectively zero, because one can (roughly speaking) obtain a history with equally good fit by moving ancestors from that time interval into the neighboring ones, resulting in peaks on either side of the selected time interval. Thus, these lower bounds are perhaps unrealistic, and the reader should bear in mind that the dependence between intervals in our uncertainty is not depicted.

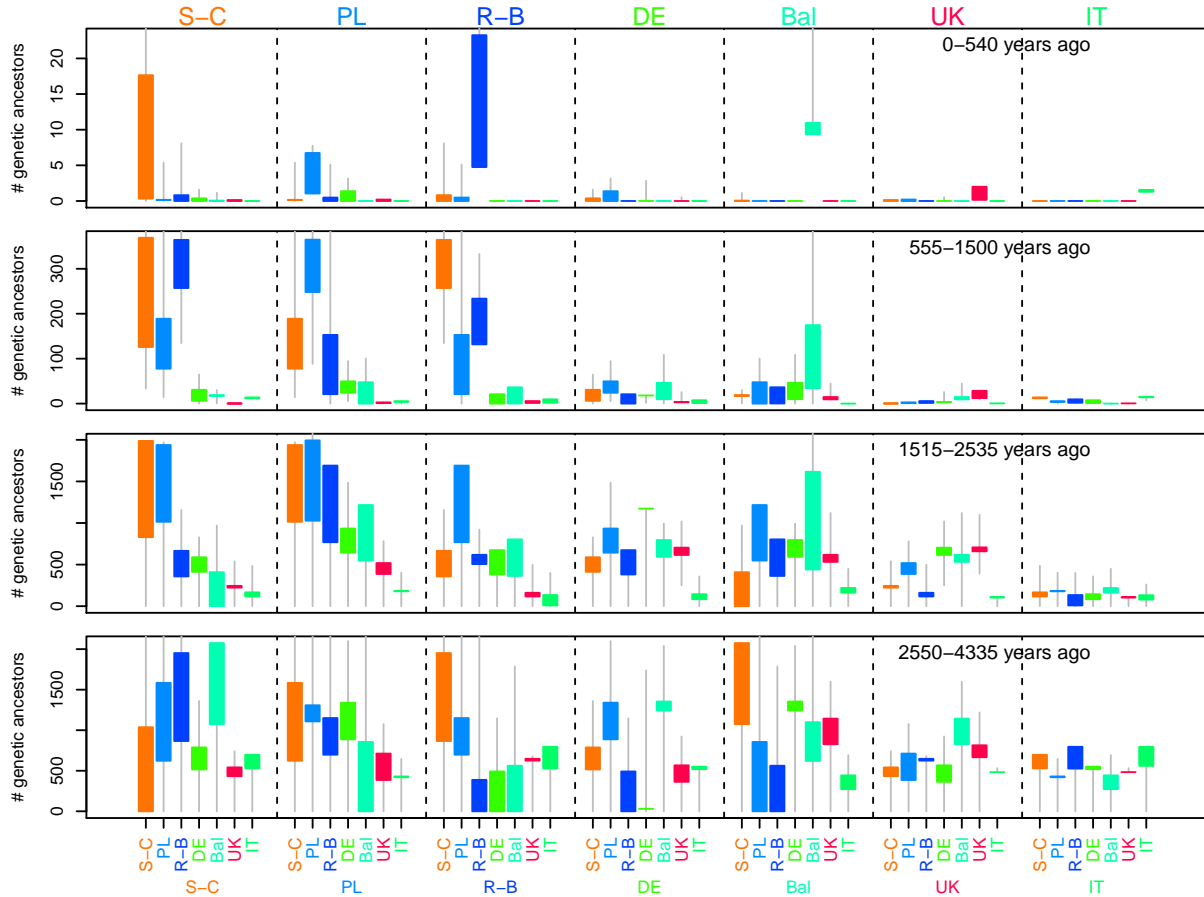


Figure 5: Estimated total numbers of genetic common ancestors shared by various pairs of populations, in roughly the time periods 0–500ya, 500–1500ya, 1500–2500ya, and 2500–4300ya. We have combined some populations to obtain larger sample sizes: “S-C” denotes Serbo-Croatian speakers in former Yugoslavia, “PL” denotes Poland, “R-B” denotes Romania and Bulgaria, “DE” denotes Germany, “Bal” denotes Latvia, Finland, Sweden, Norway, and Denmark, “UK” denotes the United Kingdom, and “IT” denotes Italy. For instance, the green bars in the leftmost panels tell us that Serbo-Croatian speakers and Germans share 0–1 most recent genetic common ancestor from the last 500 years, 10–30 from the period 500–1500 years ago, and around 500 from each of the two previous thousand years. Although the lower bounds appear to extend to zero, they are significantly above zero in nearly all cases except for the most recent period 0–540ya.

Results of age inference In figure 4 we show how the age and amount of shared genetic ancestry changes as we move away from the Balkans (left column) and the UK (right column), along with two examples of how the observed block length distribution is composed of ancestry from different depths. More plots of this form are shown in supplemental figure S7.

Most detectable recent common ancestors lived between 1500 and 2500 years ago. Furthermore, only a

small proportion of blocks longer than 2cM are inherited from longer ago than 4000 years. Obviously, there are a vast number of genetic common ancestors older than this, but the blocks inherited from such common ancestors are sufficiently unlikely to be longer than 2cM that we do not detect many. For the most part, blocks longer than 4cM come from 500–1500 years ago, and blocks longer than 10cM from the last 500 years.

In most cases, only pairs within the same population are likely to share genetic common ancestors within the last 500 years. Exceptions are generally neighboring populations that have had high population growth and/or asymmetric migration rates recently (e.g. UK and Ireland). During the period 500–1500ya, individuals typically share tens to hundreds of genetic common ancestors with others in the same or nearby populations, although some distant populations have very low rates. Longer ago than 1500ya, pairs of individuals from any part of Europe share hundreds of genetic ancestors in common, and some share significantly more.

Regional variation: interesting cases We now examine some of the more striking patterns we see in more detail.

There is relatively little common ancestry shared between the Italian peninsula and other locations, and what there is seems to derive from longer ago than 2500ya. This relatively old date is consistent with the weak relationship of geographic distance and rate of IBD sharing of figure 3, as discussed above. An exception is that Italy and the neighboring Balkan populations share small but significant numbers of common ancestors in the last 1500 years, as seen in supplemental figures S7 or S8. The rate of genetic common ancestry between pairs of Italian individuals seems to have been fairly constant for the past 2500 years, which combined with significant structure within Italy suggests a constant exchange of migrants between coherent subpopulations. Also recall that most populations show no substructure with regards the number of blocks shared with Italians, implying that the common ancestors shared with Italy predate divisions within these populations.

Patterns for the Iberian peninsula are similar, with both Spain and Portugal showing very few common ancestors with other populations over the last 2500 years. However, the rate of IBD sharing within the peninsula is much higher than within Italy – the Iberian peninsula shares fewer than 5 genetic common ancestors with other populations during the last 1500 years, compared to 78 per pair within the peninsula, and past 1500ya Iberian individuals share only slightly more genetic common ancestors with each other as they do with people from most of the rest of Europe.

The higher rates of IBD between populations in the “E” grouping shown in figure 3 seem to derive mostly from ancestors living 1500–2500ya, but also show increased numbers from 500–1500ya, as shown in figure 5 and supplemental figures S8. Across all populations, even geographically distant individuals share about as many common ancestors as do two Irish or two French-speaking Swiss.

By far the highest rates of IBD within any populations is found between Albanian speakers – around 200 ancestors from 0–500ya, and around 1800 ancestors from 500–1500ya (so high that we left them out of figure 5; see supplemental figure S5). Beyond 1500ya, the rates of IBD drop to levels typical for other populations in the eastern grouping.

There are clear differences in the number and timing of genetic common ancestors shared by individuals from different parts of Europe. These differences reflect the impact of major historical and demographic events, superimposed against a background of local migration and generally high genealogical relatedness across Europe. We now turn to discuss possible causes and implications of these results.

3 Discussion

Genetic common ancestry within the last 2,500 years across Europe has been shaped by diverse demographic and historical events. There are both continental trends, such as a decrease of shared ancestry with distance, regional patterns, such as higher IBD in eastern and northern populations, and diverse outlying signals. We have furthermore quantified numbers of genetic common ancestors that populations share with each other back through time, albeit with a large degree of (unavoidable) uncertainty. These numbers are intriguing not only because of the differences between populations, which reflect historical events, but the high degree of implied commonality between even geographically distant populations.

Ubiquity of common ancestry We have shown that typical pairs of individuals drawn from across Europe have a good chance of sharing long stretches of identity by descent, even when they are separated by thousands of kilometers. This implies that pairs of individuals across Europe likely share common genetic ancestors within the last 1,000 years, and are certain to share many within the last 2,500 years. The average number of genetic common ancestors from the last 1,000 years shared by individuals living at least 2,000km apart is about .125 (and at least .05); between 1,000–2,000ya they share about four; and between 2,000–3,000ya they share above 50. Since the chance is small that any genetic material has been transmitted along a particular genealogical path from ancestor to descendent more than 8 generations deep (Donnelly, 1983) – about .008 at 240ya, and 2.5×10^{-7} at 480ya – this implies the sharing of, conservatively, thousands of genealogical ancestors in only the last 1,000 years between pairs of individuals even when they are separated by large geographic distances. At first sight this result seems counterintuitive. However, as 1000 years is about 33 generations, and $2^{33} \approx 10^{10}$ is far larger than the size of the European population, so long as populations have mixed sufficiently, by 1,000 years ago everyone (who left descendants) would be an ancestor of every present day European. Our results are therefore one of the first genomic demonstrations of the counter-intuitive but necessary fact that all Europeans are genealogically related over very short time periods, and lends substantial support to models predicting close and ubiquitous common ancestry of all modern humans (Rohde et al., 2004).

The fact that most people alive today in Europe shares nearly the same set of (European, and possibly world-wide) ancestors from only 1,000 years ago seems to contradict the signals of long term, albeit subtle, population genetic structure within Europe (e.g. Novembre et al., 2008; Lao et al., 2008). These two facts can be reconciled by the fact that even though the distribution of ancestors (as cartooned in Figure 1B) has spread to cover the continent, there remain differences in degree of relatedness of modern individuals to these ancestral individuals. For example, someone in Spain may be related to an ancestor in the Iberian peninsula through perhaps 1000 different routes back through the pedigree, but to an ancestor in the Baltic region by only 10 different routes, so that the probability that this Spanish individual inherited genetic material from the Iberian ancestor is 100 times higher. This allows the amount of genetic material shared by pairs of extant individuals to vary even if the set of ancestors is constant.

Limitations of Sampling A concern about our results is that the European individuals in the POPRES dataset were all sampled in either Lausanne or London. This might bias our results, for instance, because immigrant communities may originate mostly from a particular small portion of their home population, thereby sharing a particularly high number of common ancestors with each other. We see remarkably little evidence that this is the case: there is a high degree of consistency in numbers of IBD blocks shared across samples from each population, and between neighboring populations. For instance, the high degree of shared common ancestry among Albanian speakers might be because most of these originated from a small village rather than uniformly across Albania and Kosovo. However, this would not explain the high rate of IBD between Albanian speakers and neighboring populations. Even populations from which we only have one or two samples, which we at first assumed would be unusably noisy, provide generally reliable, consistent patterns, as evidenced by e.g. supplemental figure S3.

Conversely, it might be a concern that individuals sampled in Lausanne or London are more likely to have recent ancestors more widely dispersed than is typical for their population of origin. This is a possibility we cannot discard, and if true, would mean there is more structure within Europe than what we detect. However, again by the incredibly rapid spread of ancestry, this is unlikely to have an effect over more than a few generations and so does not pose a serious concern about our results. Fine-scale geographic sampling of Europe as a whole is needed to address these issues, and these efforts are underway in certain populations (e.g. Price et al., 2009; Jakkula et al., 2008; Tyler-Smith and Xue, 2012; Winney et al., 2011).

Finally, we have necessarily have taken a narrow view of European ancestry as we have restricted our sample to individuals who are not outliers with respect to genetic ancestry, and when possible to those having all four grandparents drawn from the same county. Clearly the ancestry of Europeans is far more diverse than those represented here, but such steps seemed necessary to make best use of this dataset.

Ages of particular common ancestors We have shown that the problem of inferring the average distribution of genetic common ancestors back through time has a large degree of fundamental uncertainty. The data effectively leave a large number of degrees of freedom unspecified, so one must either describe the set of possible histories, as we do, and/or use prior information to restrict these degrees of freedom.

A related but far more intractable problem is to make a good guess of how long ago a *certain* shared genetic common ancestor lived, as personal genome services would like to do, for instance: if you and I share a 10cM block of genome IBD, when did our most recent common ancestor likely live? Since the mean length of an IBD block inherited from 5 generations ago is 10cM, we might expect the average age of the ancestor of a 10cM block to be from around 5 generations. However, using our results, the typical age of a 10cM block shared by two individuals from the UK is between 32 and 52 generations. This discrepancy results from the fact that you are *a priori* much more likely to share a common genetic ancestor further in the past, and this acts to skew our answers away from the naive expectation. This also means that estimated ages must depend drastically on the populations’ shared histories: the age of such a block shared by someone from the UK with someone from Italy is older, usually from 56 to 60 generations ago. This may not apply to ancestors from the past very few (perhaps less than eight) generations, from whom we expect to inherit multiple long blocks – in this case we can hope to infer a specific genealogical relationship with reasonable certainty (e.g. Huff et al., 2011; Henn et al., 2012b), although even then care must be taken to exclude the possibility that these multiple blocks have not been inherited from distinct common ancestors.

Although the sharing of a long genomic segment can be an intriguing sign of some recent shared ancestry, the ubiquity of shared genealogical ancestry only tens of generations ago across Europe (and likely the world, Rohde et al., 2004) makes such sharing unsurprising, and assignment to particular genealogical relationships impossible. What is informative about these chance sharing events from distant ancestors is that they provide a fine-scale view of an individual’s distribution of ancestors (e.g. figure 3), and that in aggregate they can provide an unprecedented view into even small-scale human demographic history.

3.1 The signal of history

As we have shown, patterns of IBD provide ample but noisy geographic and temporal signals, which can then be connected to historical events. Rigorously making such connections is difficult, due to the complex recent history of Europe, controversy about the demographic significance of many events, and uncertainties in inferring the ages of common ancestors. Nonetheless, our results can be plausibly connected to several historical and demographic events.

The migration period – Huns, Goths, and Slavs One of the striking patterns we see is the relatively high level of sharing of IBD between pairs of individuals across eastern Europe, as high or higher than that observed within other, much smaller populations. Furthermore, the numbers of short (older) IBD blocks shared between different populations is constant regardless of the geographic distance separating the two, as shown in figure 3. This is consistent with these individuals having a comparatively large proportion of ancestry drawn from a relatively small population that expanded over a large geographic area, ancestry which we date to 1,000–2,000 years ago (see figures 4, 5, and S8). For example, even individuals from widely separated eastern populations share about the same amount of IBD as do two Irish individuals (see supplemental figure S3), suggesting that this ancestral population may have been relatively small.

This evidence is consistent with the idea that these populations derive a substantial proportion of their ancestry from various groups that expanded during the “migration period” from the fourth through ninth centuries (Davies, 2010). This period begins with the Huns moving into eastern Europe towards the end of the fourth century, establishing an empire including modern-day Hungary and Romania; and continues in the fifth century as various Germanic groups moved into and ruled much of the western Roman empire. The Slavic populations expanded beginning in the sixth century, probably from somewhere in the area between the Baltic, Black, and Adriatic seas (Barford, 2001). By the seventh century, Slavic groups had spread into the Balkan Peninsula, and occupied much of the northern Balkans by the 10th century. The inclusion of (non-Slavic speaking) Hungary and Romania in the group of eastern populations sharing high IBD could be

due to the Huns, or because some of the same group of people who elsewhere are known as Slavs adopted different local cultures in those regions. Greece and Albania are also part of this putative signal of expansion, which could be because the Slavs settled in part of these areas (with unknown demographic effect). Additional work and methods would be needed to ascertain the geographic source(s) of this expansion.

Italy, Iberia, and France On the other hand, we find that France and the Italian and Iberian peninsulas have the lowest rates of genetic common ancestry in the last 1,500 years, other than Turkey and Cyprus, and are the regions of continental Europe thought to be least affected by the Slavic and Hunnic migrations. These regions were, however, moved into by Germanic tribes (e.g. the Goths, Ostrogoths, and Vandals), which suggests that perhaps the Germanic migrations/invasions of these regions entailed a smaller degree of population replacement, or at least a larger rate of population growth, than the Slavic and/or Hunnic. It has been argued that this is the case, perhaps because Slavs moved into relatively depopulated areas, while Gothic “migrations” may have been takeovers by small military groups of extant populations (Halsall, 2005; Kobyliński, 2005).

In addition to the very few genetic common ancestors that Italians share both with each other and with other Europeans, we have seen significant modern substructure within Italy (i.e. figure 2) that predates most of this common ancestry, and estimate that most of the common ancestry shared between Italy and other populations is older than about 2,300 years (i.e. supplemental figure S7). This suggests significant substructure and large population sizes within Italy, strong enough that different groups within Italy, share as little recent common ancestry as other distinct, modern-day countries, substructure that was not homogenized during the migration period. These patterns could also reflect in part a history of settlement of Italy from various sources, including: settlement of Greeks in southern Italy, settlement of Illyrians in eastern Italy, and an influx of people from across the Roman empire, including gene flow from Africa (Auton et al., 2009; Moorjani et al., 2011); but is unlikely to be entirely due to these effects.

In contrast to Italy, the rate of sharing of IBD within the Iberian peninsula is similar to that within other populations in Europe. There is furthermore much less evidence of substructure within our Iberian samples than within the Italians, as shown in supplemental figure S2. This suggests that the reduced rate of shared ancestry is due to geographic isolation (by distance and/or the Pyrenees) rather than stable substructure within the peninsula. While the African gene flow into Iberia has likely reduced the amount of sharing with the rest of Europe, as it contributed only a few percent of the ancestry of modern genomes (Moorjani et al., 2011), it cannot explain the size of the reduction that we see. Furthermore, most of the shared ancestry between the Iberian peninsula and other populations seems to have occurred more than 2,000 years ago. It seems therefore that the Germanic (and later Moorish) invasions did not lead to increased common ancestry in the same way as the expansions in eastern Europe, and that subsequent mixing was slowed by geography.

Other historical signals There are many other possible signals in these data, here we focus on only a few.

The highest levels of IBD sharing are found in the Albanian-speaking individuals (from Albania and Kosovo), an increase in common ancestry deriving from the last 1,500 years. This suggests that a reasonable proportion of the ancestors of modern-day Albanian speakers are drawn from a relatively small, cohesive population that has persisted for at least the last 1,500 years. These individuals share similar numbers of common ancestors with nearby populations as do individuals in other parts of Europe, implying that the Albanian speakers have not been a particularly isolated population so much as a small one. Furthermore, our Greek samples (and to a lesser degree, the Macedonians) share much higher numbers of common ancestors with Albanian speakers than with other neighbors, possibly due to smaller effects of the Slavic expansion in these populations. The Albanian language is an Indo-European language without other close relatives (Hamp, 1966) that persisted through periods when neighboring languages were strongly influenced by Latin or Greek. The “origin” of modern-day Albanians is contentious; it is argued for instance that they are descended in large part from the Illyrians (Wilkes, 1996) who populated the eastern side of the Adriatic sea and part of modern-day Salento (Italy) during Roman times. Our results are certainly consistent with this view, including the fact that Italians share more common ancestors with Albanian speakers than with other

populations (although these ancestors are estimated to be from the last 1,500 years), so this may reflect more recent migration.

There are other regions having high genetic common ancestry that suggest intriguing conclusions, but must remain tentative due to low sample sizes. For example, our 13 samples from Scandinavian populations (Norway, Sweden, Denmark) share high rates of IBD with each other and with certain nearby populations. We estimate that these populations had higher rates of genetic common ancestry from the last 1500 years with the UK, Ireland, Belgium, the Netherlands, France, Germany, German-speaking Swiss, Finland, Russia, Latvia, Romania, and Ukraine (see supplemental figure S5), which coincides quite well with known Viking settlements, suggesting that the Norse expansion may have had a significant demographic effect. However, we would need larger samples to be confident about these results.

Future directions Our results show that patterns of recent identity by descent both provide evidence of ubiquitous shared common ancestry and hold the potential to shed considerable light on the complex history of Europe. However, these inferences also quickly run up against a fundamental limit to our ability to infer pairwise rates of recent common genetic ancestry. In order to make a fuller model of European history, we will need to make use of diverse sources of genomic information from large samples, including IBD segments and rare variants (Nelson et al., 2012; Tennessen et al., 2012), and develop methods that can more fully utilize this information. Another profound difficulty is that Europe – and indeed any large continental region – has such complex layers of history, through which ancestry has mixed so greatly, that attempts to connect genetic signals in extant individuals to particular historical events requires the corroboration of other sources of information. For example, the ability to isolate ancient autosomal DNA from individuals who lived during these time periods (as do Skoglund et al., 2012; Keller et al., 2012) will help to overcome some of these profound difficulties. More generally, the quickly falling cost of sequencing, along with the development of new methods, will shed light on the recent demographic and genealogical history of populations of recombining organisms, human and otherwise.

4 Materials and Methods

4.1 Description of data and data cleaning

The portion of the POPRES dataset that we use was collected partly in Lausanne, Switzerland and partly in London, England; it is described in Nelson et al. (2008). Those collected in Lausanne reported parental and grandparental country of origin; those collected in London did not. We followed Novembre et al. (2008) in assigning each sample to the common grandparental country of origin when available, and discarding samples whose parents or grandparents originated from different countries. We took further steps to restrict to individuals whose grandparents came from the same geographic region, first performing principal components analysis on the data using SMARTPCA (Patterson et al., 2006), and excluding those individuals who clustered with populations outside Europe (the majority of such were already excluded by self-reported non-European grandparents). We then used PLINK’s inference of the fraction of single-marker IBD (Z0, Z1, and Z2, Purcell et al., 2007) to identify very close relatives, finding 25 pairs that are first cousins or closer (including duplicated samples), and excluded one individual from each pair. We grouped samples into populations mostly by reported country, but also used reported language in a few cases. Because of the large Swiss samples, we split this group into three by language: French-speaking (CHf), German-speaking (CHd), or other (CH). Many samples reported grandparents from Yugoslavia; when possible we assigned these to a modern-day country by language, and when this was ambiguous or missing we assigned these to “Yugoslavia”. Most samples from the United Kingdom reported this as their country of origin; however, the few that reported “England” or “Scotland” were assigned this label. This left us with 2,257 individuals from 40 populations; for sample sizes see table 1. Supplemental table S1 further breaks this down, and unambiguously gives the composition of each population. Physical distances were converted to genetic distances using the hg36 map, and the average human generation time was taken to be 30 years (Fenner, 2005).

Code implementing all methods described below are available at <http://www.github.com/petrelharp>.

4.2 Calling IBD blocks

To find blocks of IBD, we used the method **fastIBD** implemented in **BEAGLE** (Browning and Browning, 2011). As suggested by the authors, in all cases we ran the algorithm 10 times with different random seeds, and postprocessed the results to obtain IBD blocks. Based on our power simulations described below, we modified the postprocessing procedure recommended by Browning and Browning (2011) to deal with spurious gaps introduced into long blocks of IBD. We called IBD segments by first removing any segments not overlapping a segment seen at least one other run (with no score cutoff); then merging any two segments separated by a gap shorter than at least one of the segments and no more than 5cM long; and finally discarding any merged segments that did not contain a subsegment with score below 10^{-9} . As shown in figure 6, this resulted in a false positive rate of between 8–15% across length categories, and a power of at least 70% above 1cM, reaching 95% by 4cM. After post-processing, we were left with 1.9 million IBD blocks, 1 million of which were at least 2cM long (at which length we estimate 85% power and a 10% false positive rate).

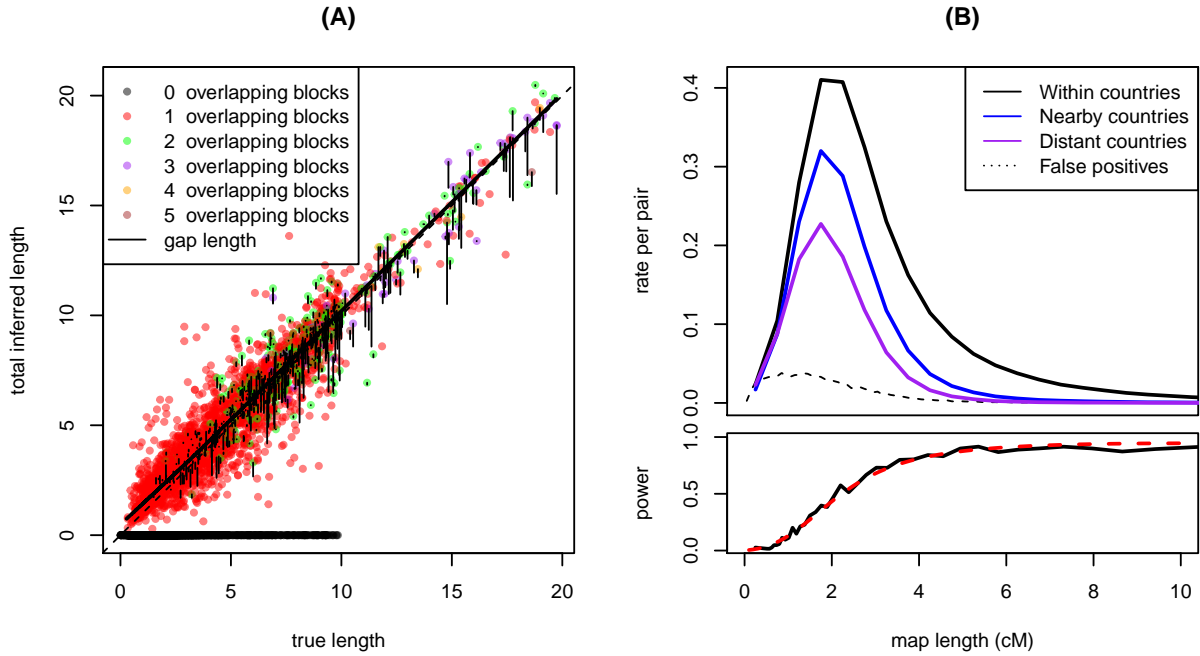


Figure 6: (A) Bias in inferred length with lines $x = y$ (dotted) and a **loess** fit (solid). Each point is a segment of true IBD (copied between individuals), showing its true length and inferred length after postprocessing. Color shows the number of distinct, nonoverlapping segments found by BEAGLE, and the length of the vertical line gives the total length of gaps between such segments that BEAGLE falsely inferred was not IBD. (B) Estimated false positive rate as a function of length. Observed rates of IBD blocks, per pair and per cM, are also displayed for the purpose of comparison. “Distant” and “Nearby” means IBD between pairs of populations closer and farther away than 1000km, respectively. (C) Below, the estimated power as a function of length, together with the parametric fit of equation (5).

4.3 Power and false positive simulations

All methods to identify haplotypic IBD rely on identifying long regions of near identical haplotypes between pairs of individuals (referred to as identical by state, IBS). However, long IBS haplotypes could potentially also result from the concatenation of multiple shorter blocks of true IBD. While such runs can contain important information about deeper population history (e.g. Li and Durbin, 2011), we view them as a false positives as they confound our relationships between number of shared IBD blocks and genetic ancestors. The chance of such a false positive IBD segment decreases as the genetic length of shared haplotype increases. However, the density of informative markers also plays a role, because in regions of low marker density we can miss alleles that differ.

If we are to have a reasonable false positive rate, we must accept imperfect power. Power will also vary with the density and informativeness of markers and length of segment considered. For example, it is intuitive that segments of genome containing many rare alleles are easier identify as IBD. Conversely, rare immigrant segments from a population with different allele frequencies may have higher false positive rates. For these reasons, when estimating statistical power and false positive rate, it is important to use a dataset as similar to the one under consideration as possible. Therefore, to determine appropriate postprocessing criteria and to estimate our statistical power, we constructed a dataset similar to the POPRES with known shared IBD segments as follows: we copied segments randomly between 60 trio-phased individuals of European descent (using only one from each trio) from the HapMap dataset (haplotypes from release #21, 17/07/06 International HapMap Consortium et al., 2007), substituted these for 60 individuals from Switzerland in the POPRES data, and ran BEAGLE on the result as before. We copied segments of single chromosomes between randomly chosen individuals, for random lengths 0.5–20cM, with gaps of at least 2cM between adjacent segments and without copying between the same two individuals twice in a row. When copying, we furthermore introduced genotyping error by flipping alleles independently with probability .002 and marking the allele missing with probability .023 (error rates were determined from duplicated individuals in the sample). An important feature of the inferred data was that BEAGLE often missed gaps in blocks longer than about 5cM, which led us to merge blocks as described above.

We need a reasonably accurate assessment of our power, bias, and false positive rates for our inversion of the relationship between IBD block rate and number of genetic ancestors. Although the estimated IBD lengths were approximately unbiased, to adjust equation (8) we also fit a parametric model to the relationship between true and inferred lengths after removing inferred blocks less than 1cM long. A true IBD block of length x is missed entirely with probability $1 - c(x)$, and is otherwise inferred to have length $x + \epsilon$; with probability $\gamma(x)$ the error ϵ is positive; otherwise it is negative and conditioned to be less than x . In either case, ϵ is exponentially distributed; if $\epsilon > 0$ its mean is $1/\lambda_+(x)$, while if $\epsilon < 0$ its (unconditional) mean is $1/\lambda_-(x)$. The parametric forms were chosen by examination of the data, and fit by maximum likelihood; these are:

$$c(x) = 1 - 1 / (1 + .077x^2 \exp(.54x)) \quad (1)$$

$$\gamma(x) = .34 (1 - (1 + .51(x - 1)^+ \exp(.68(x - 1)^+))^{-1}) \quad (2)$$

$$\lambda_+(x) = 1.40 \quad (3)$$

$$\lambda_-(x) = \min(.40 + 1/ (.18x), 12) \quad (4)$$

where $z^+ = \max(z, 0)$.

To estimate the false positive rate, we randomly shuffled segments of diploid genome between individuals from the same population (only those 12 populations with at least 19 samples) so that any run of IBD longer than about 0.5cM would be broken up among many individuals. Specifically, as we read along the genome we output diploid genotypes in random order; we shuffled this order by exchanging the identity of each output individual with another at independent increments chosen uniformly between 0.1 and 0.2cM. This ensured that no output individual had a continuous run of length longer than 0.2cM copied from a single input individual, while also preserving linkage on scales shorter than 0.1cM. The results are shown in figure 6B; from these we estimate that the mean density of false positives x cM long per pair and per cM is

approximately

$$f(x) = \exp(-13 - 2x + 4.3\sqrt{x}), \quad (5)$$

a parametric form again chosen by examination of the data.

4.4 IBD rates along the genome

To look for regions of unusual levels of IBD and to examine our assumption of uniformity, we compared the density of IBD tracts of different lengths along the genome, in supplemental figure S1. To do this, we first divided blocks up into nonoverlapping bins based on length, with cutpoints at 1, 2.5, 4, 6, 8, and 10cM. We then computed at each SNP the number of IBD blocks in each length bin that covered that site. To control for the effect of nearby SNP density on the ability to detect IBD, we then computed the residuals of a linear regression predicting number of overlapping IBD blocks using the density of SNPs within 3cM. To compare between bins, we then normalized these residuals, subtracting the mean and dividing by the standard deviation; these “z-scores” for each SNP are shown in figure S1.

4.5 Correlations in IBD rates

We noted repeated patterns of IBD sharing across multiple populations (seen in supplemental figure S3), in which certain sets of populations tended to show similar patterns of sharing. To quantify this, we computed correlations between mean numbers of IBD blocks of various lengths; in supplemental figure S4 we show correlations in numbers blocks of various lengths. Specifically, if $I(x, y)$ is mean the number of IBD blocks of the given length shared by an individual from population x with a (different) individual from population y , there are n populations, and $\bar{I}(x) = (1/(n-1)) \sum_{y \neq x} I(x, y)$, then figure S4 shows for each x and y ,

$$\frac{1}{n-2} \sum_{z \notin \{x, y\}} (I(x, z) - \bar{I}(x))(I(y, z) - \bar{I}(y)), \quad (6)$$

the (Pearson) correlation between $I(x, z)$ and $I(y, z)$ ranging across $z \notin \{x, y\}$. Other choices of block lengths are similar, although shorter blocks show higher overall correlations (due in part to false positives) and longer blocks show lower overall correlations (as rates are noisier, and sharing is more restricted to nearby populations). The groups were then chosen by visual inspection.

4.6 Substructure

We also assessed overall degrees of substructure within populations, i.e. the degree of inhomogeneity across individuals of population x for shared ancestry with population y (relative to that expected by chance). We measured inhomogeneity by the standard deviation in number of blocks shared with population y , across individuals of population x . We assessed the significance relative to a model of no substructure by a permutation test, randomly reassigning each block shared between x and y to a individual chosen uniformly from population x , and recomputing the standard deviation, 1000 times. The resulting p -values are shown in supplemental figure S2. We did not analyze these in detail, particularly as we had limited power to detect substructure in populations with few samples, but note that a large proportion (47%) of the population pairs showed greater inhomogeneity than in all 1000 permuted samples (i.e. $p < .001$). Some comparisons even with many samples in both populations showed no structure whatsoever – in particular, the distribution of numbers of Italian IBD blocks shared by Swiss individuals is not distinguishable from Poisson, indicating a high degree of homogeneity of Italian ancestry across Switzerland.

4.7 Inferring ages of common ancestors

Here, our aim is to use the distribution of IBD block lengths to infer how long ago the genetic common ancestors were alive from which these IBD blocks were inherited. A pair of individuals who share a block of IBD of genetic length at least x have each inherited contiguous regions of genome from a single common

ancestor n generations ago, and these regions overlap for length at least x . The common ancestors of two individuals from which they might have inherited IBD blocks are those that can be connected to both by paths through the pedigree. Each link in such a path represents a meiosis (i.e. a reproduction) through which a certain amount of genetic material is passed, and the number of meioses is what determines the distribution of possible IBD blocks.

Throughout the article we informally often refer to ancestors living a certain “number of generations in the past” as if humans were semelparous with a fixed lifetime (Fenner, 2005, of roughly 30 years). Keeping with this, it is natural to write the number of IBD blocks shared by a pair of individuals as the sum over past generations of the number of IBD blocks inherited from that generation. More carefully, if $N(x)$ is the number of IBD blocks of genetic length at least x shared by two individual chromosomes, and $N_n(x)$ is the number of such IBD blocks inherited by the two along paths through the pedigree with a total of n meioses, then $N(x) = \sum_n N_n(x)$. Therefore, averaging over possible choices of pairs of individuals, the mean number of shared IBD blocks can be similarly partitioned as

$$\mathbb{E}[N(x)] = \sum_{n \geq 1} \mathbb{E}[N_n(x)]. \quad (7)$$

In each successive generation in the past each chromosome is broken up into successively more pieces, each of which has been inherited along a different path through the pedigree. Returning to the semelparous example, any two such pieces of the two individual chromosomes that overlap and are inherited from the same ancestral chromosome contribute one block of IBD. Therefore, the mean number of IBD blocks coming from t generations ago is the mean number of such possibly overlapping pieces multiplied by the probability that a particular pair of these pieces are first descended from the same genealogical ancestor in generation t . Allowing for uncoordinated generations, let $K(n, x)$ denote the mean number of pieces of length at least x obtained by cutting the chromosome at the recombination sites of n meioses, and $\mu(n)$ the probability that the two chromosomes have inherited at a particular site along a path of total length n meioses (e.g. their common ancestor at that site lived $n/2$ generations ago). Then $\mathbb{E}[N_n(x)]$ is the product of these two terms, so that

$$\mathbb{E}[N(r)] = \sum_{n \geq 1} \mu(n) K(n, r), \quad (8)$$

i.e. the mean rate of IBD is a linear function of the distribution of the time back to the most recent common ancestor. The distribution $\mu(n)$ is more precisely known as the coalescent time distribution (Kingman, 1982; Wakeley, 2005), in its obvious adaptation to pedigrees.

Furthermore, it is easy to calculate that for a chromosome of genetic length G , without interference (i.e. Poisson recombination)

$$K(n, x) = (n(G - x) + 1) \exp(-xn). \quad (9)$$

The mean number of IBD blocks of length at least x shared by a pair of individuals across the entire genome is then obtained by summing (8) across all chromosomes, and multiplying by four (for the four possible chromosome pairs).

Equations (8) and (9) give the relationship between lengths of shared IBD blocks and how long ago the ancestor lived from whom these blocks are inherited. Our goal is to invert this relationship to learn about $\mu(n)$, and hence the ages of the common ancestors underlying our observed distribution of IBD block lengths. To do this, we first need to account for sampling noise and estimation error. Suppose we are looking at IBD blocks shared between any of a set of n_p pairs of individuals, and assume that $N(y)$, the number of *observed* IBD blocks shared between any of those pairs of length at least y , is Poisson distributed with mean $n_p M(y)$, where

$$M(y) = f(y) + \sum_{n \geq 1} \mu(n) \int_y^G \left(\int_0^G c(x) R(x, z) dK(n, x) \right) dz, \quad \text{with} \quad (10)$$

$$R(x, y) = \begin{cases} \gamma(x) \lambda_+(x) \exp(\lambda_+(x)(y - x)) & \text{for } y > x \\ (1 - \gamma(x)) \lambda_- \exp(\lambda_-(x)(x - y)) / (1 - \exp(\lambda_-(x)x)) & \text{for } y < x. \end{cases} \quad (11)$$

Here the power $c(x)$ and the components of the error kernel $R(x, y)$ are estimated as above. The Poisson assumption is reasonable because there is a very small chance of having inherited a block from each pair of shared genealogical ancestors; there a great number of these, and if these events are sufficiently independent, the Poisson distribution will be a good approximation (see e.g. Grimmett and Stirzaker, 2001). If this holds for each pair of individuals, the total number of IBD blocks is also Poisson distributed, with M given by the mean of this number across all constituent pairs.

Unfortunately, the problem is ill-conditioned (the canonical example is the Laplace transform Epstein and Schotland, 2008), which in this context means that the likelihood surface is flat in certain directions (“ridged”): for each IBD block distribution $N(x)$ there is a large set of coalescent time distributions $\mu(n)$ that fit the data equally well. A common problem in such problems is that the unconstrained maximum likelihood solution is wildly oscillatory; in our case, the unconstrained solution is not so obviously wrong, since we are helped considerably by the knowledge that $\mu \geq 0$. For reviews of approaches to such ill-conditioned inverse problems, see e.g. Petrov and Sizikov (2005) or Stuart (2010); the problem is also known as “data unfolding” in particle physics (Cowan, 1998). If one is concerned with finding a point estimate of μ , most approaches add an additional penalty to the likelihood, which is known as “regularization” (Tikhonov and Arsenin, 1977) or “ridge regression” (Hoerl and Kennard, 1970). However, our goal is parametric inference, and so we must describe the limits of the “ridge” in the likelihood surface in various directions, (which can be seen as maximum *a posteriori* estimates under priors of various strengths).

To do this, we first discretize the data, so that N_i is the number of IBD blocks with inferred genetic lengths falling between x_{i-1} and x_i , with a minimum length of $2cM$ long, so that $x_0 = 2$. We then compute by numerical integration the matrix L discretizing the kernel given in (10), so that $L_{in} = \int_{x_{i-1}}^{x_i} \int_0^G c(x)R(x, z)dK(n, x)dz$ is the kernel that applied to μ gives the mean number of true IBD blocks per pair observed with lengths between x_{i-1} and x_i , and $f_i = \int_{x_{i-1}}^{x_i} f(z)dz$ is the mean number of false positives per pair with lengths in the same interval. We then sum across chromosomes, as before. The likelihood of the data is thus

$$\exp\left(-\sum_i L_{in}\mu_n - f_i\right) \prod_i \frac{1}{N_i!} (L_{in}\mu_n + f_i)^{N_i} \quad (12)$$

To the (negative) log likelihood we add a penalization γ , and use numerical optimization (`optim` in R Development Core Team, 2012) to minimize the resulting functional (which omits terms independent of μ)

$$\mathcal{L}(\mu; \gamma, N) = \sum_i L_{in}\mu_n - \sum_i \frac{N_i}{n_p} \log(L\mu + f)_i + \frac{\gamma(\mu)}{n_p}. \quad (13)$$

Often we will fix the functional form of the penalization and vary its strength, so that $\gamma(\mu) = \gamma_0 z(\mu)$, in which case we will write $\mathcal{L}(\mu; \gamma_0, N)$ for $\mathcal{L}(\mu; \gamma_0 z(\mu), N)$.

For instance, the leftmost panels in figure 4 show the minimizing solutions μ for $\gamma = 0$ (no penalization) and for $\gamma = \gamma_0 \sum_n (\mu_{n+1} - \mu_n)^2$ (“roughness” penalization). Because our aim is to describe extremal reasonable estimates μ , in this and in other cases, we have chosen the strength of penalization γ_0 to be “as large as is reasonable”, choosing the largest γ_0 such that the minimizing μ has log likelihood differing by no more than 2 units from the unconstrained optimum. This choice of cutoff can be justified as in Edwards (1984), and gave quite similar answers to other methods. This can be thought of as taking the strongest prior that still gives us “reasonable” maximum *a posteriori* answers. Note that the optimization is over *nonnegative* distributions μ also satisfying $\sum_n \mu(n) \leq 1$ (although the latter condition does not enter in practice).

We would also like to determine bounds on total numbers of shared genetic ancestors who lived during particular time intervals, by determining e.g. the minimum and maximum numbers of such ancestors that are consistent with the data. Such bounds are shown in figure 5. To obtain a lower for the time period between n_1 and n_2 generations, we penalized the total amount of shared ancestry during this interval, using the penalizations $\gamma_-(\mu) = \gamma_0^- (\sum_{n=n_1}^{n_2} \mu(n))^2$, and choosing γ_0^- to give a drop of 2 log likelihood units, as described above. The lower bound is then the total amount of coalescence $\sum_{n=n_1}^{n_2} \mu_-(n)$ for μ_- minimizing

$\mathcal{L}(\cdot; \gamma_-, N)$. The upper bound is found by penalizing total shared ancestry *outside* this interval, i.e. by applying the penalization $\gamma_+(\mu) = \gamma_0^+ (\sum_{n < n_1} \mu(n) + \sum_{n > n_2} \mu(n))^2$. It is almost always the case that lower bounds are zero, since there is sufficient wiggle room in the likelihood surface to explain the observed block length distribution using peaks just below n_1 and above n_2 . Examples are shown in supplemental figure S6. On the other hand, upper bounds seem fairly reliable.

In the above we have assumed that the minimizer of \mathcal{L} is unique, thus glossing over e.g. finding appropriate starting points for the optimization. In practice, we obtained good starting points by solving the natural approximating least-squares problem, using `quadprog` (Turlach and Weingessel, 2011) in R. We then evaluated uniqueness of the minimizer by using different starting points, and found that if necessary, adding only a very small penalization term was enough to ensure convergence to a unique solution. We furthermore produced simulated data using a variety of distributions of common ancestors, confirming that the method behaves as expected (results not shown).

Extending to shorter blocks We only used blocks longer than 2cM to infer ages of common ancestors, in part because the model we use does not seem to fit the data below this threshold. Attempts to apply the methods to all blocks longer than 1cM reveals that there is no history of rates of common ancestry that, under this model, produces a block length distribution reasonably close to the one observed – small, but significant deviations occur in the rates of short blocks. This occurs probably in part because our estimate of false positive rate is expected to be less accurate at these short lengths. Furthermore, our model does not explicitly model the overlap of multiple short IBD segments to create on long segment deriving from different ancestors, which could start to have a significant effect at short lengths. (The effect on long blocks we model as error in length estimation.) This could be incorporated into a model (in a way analogous to Li and Durbin (2011)), but consideration of when several contiguous blocks of IBD might have few enough differences to be detected as a long IBD block quickly runs into the need for a model of IBD detection, which we necessarily treat as a black box. Use of these shorter blocks, which would allow inference of older ancestry, will need different methods, and probably sequencing rather than genotyping data.

4.8 Numbers of common ancestors

Estimated numbers of genetic common ancestors can be found by simply solving for $N(0)$ using an estimate of μ in equations (8) and (9) (still restricting to genetic ancestors on the autosomes). These tell us that given the distribution $\mu(n)$, the mean number of genetic common ancestors coming from generation n – i.e. the mean number of IBD blocks of *any* length inherited from such common ancestors – is $N(0) = \mu(n) \sum_{k=1}^{22} (rnG_k + 1)$, where G_k is the total genetic length of the k^{th} human chromosome. Since the total map length of the human autosomes is about 32 Morgans, this is about $\mu(n)(32n + 22)$. This procedure has been used in figures 4 and 5.

Converting shared IBD blocks to numbers of shared *genealogical* common ancestors is more problematic. Suppose that modern-day individuals a and b both have c as a grand $^{n-1}$ parent. Using equation (9) at $x = 0$, we know that the mean number of blocks that a and b both inherit from c is $r(2n)$, with $r(n) := 2^{-n}(32n + 22)$, since each block has chance 2^{-2n} of being inherited across $2n$ meioses. First treat the endpoints of each distinct path of length n back through the pedigree as a grand $^{n-1}$ parent, so that everyone has exactly 2^n grand $^{n-1}$ parents, and some ancestors will be grand $^{n-1}$ parents many times over. Then if a and b share m genetic grand $^{n-1}$ parents, a moment estimator for the number of genealogical grand $^{n-1}$ parents is $m/r(n)$. However, the geometric growth of $r(n)$ means that small uncertainties in n have large effects on the estimated numbers of genealogical common ancestors – and we have large uncertainties in n .

Despite these difficulties, we can still get some order-of-magnitude estimates. For instance, we estimate that someone from Hungary shares on average about 5 genetic common ancestors with someone from the UK between 18 and 50 generations ago. Since $1/r(36) = 5.8 \times 10^7$, we would conservatively estimate that for every genetic common ancestor there are tens of millions of genealogical common ancestors. Most of these ancestors must be genealogical common ancestors many times over, but these must still represent at least thousands of distinct individuals.

Acknowledgements

Thanks to Razib Khan for several useful discussions, and to Jeremy Berg, Yaniv Brandvain, Joe Pickrell, Jonathan Pritchard, Alisa Sedghifar, and Joel Smith for useful comments on earlier drafts.

References

- A Albrechtsen, I Moltke, and R Nielsen. Natural selection and the distribution of identity-by-descent in the human genome. *Genetics*, 186(1):295–308, September 2010. doi: 10.1534/genetics.110.113977. URL <http://www.ncbi.nlm.nih.gov/pmc/articles/PMC2940294>.
- A Auton, K Bryc, A R Boyko, K E Lohmueller, J Novembre, A Reynolds, A Indap, M H Wright, J D Degenhardt, R N Gutenkunst, K S King, M R Nelson, and C D Bustamante. Global distribution of genomic diversity underscores rich complex history of continental human populations. *Genome Res*, 19(5):795–803, May 2009. doi: 10.1101/gr.088898.108. URL <http://www.ncbi.nlm.nih.gov/pubmed/19218534>.
- P.M. Barford. *The early Slavs: culture and society in early medieval Eastern Europe*. Cornell Univ Press, 2001.
- Marshall D. Brown, Chris G. Glazner, Chaozhi Zheng, and Elizabeth A. Thompson. Inferring coancestry in population samples in the presence of linkage disequilibrium. *Genetics*, 2012. doi: 10.1534/genetics.111.137570. URL <http://www.genetics.org/content/early/2012/01/23/genetics.111.137570.abstract>.
- Brian L. Browning and Sharon R. Browning. A fast, powerful method for detecting identity by descent. *American journal of human genetics*, 88(2):173–182, February 2011. ISSN 00029297. URL <http://linkinghub.elsevier.com/retrieve/pii/S0002929711000115>.
- R L Cann, M Stoneking, and A C Wilson. Mitochondrial DNA and human evolution. *Nature*, 325(6099):31–36, January 1987. doi: 10.1038/325031a0. URL <http://www.ncbi.nlm.nih.gov/pubmed/3025745>.
- Joseph Chang. Recent common ancestors of all present-day individuals. *Advances in Applied Probability*, 31:1002–1026, 1999.
- N H Chapman and E A Thompson. The effect of population history on the lengths of ancestral chromosome segments. *Genetics*, 162(1):449–458, September 2002. URL <http://www.ncbi.nlm.nih.gov/pmc/articles/PMC1462250/>.
- G. Cowan. *Statistical data analysis*. Oxford University Press, USA, 1998.
- N. Davies. *Europe: A History*. Random House, 2010. ISBN 9781407091792. URL <http://books.google.com/books?id=vD7SWb51XBAC>.
- K P Donnelly. The probability that related individuals share some section of genome identical by descent. *Theor Popul Biol*, 23(1):34–63, February 1983. URL <http://www.ncbi.nlm.nih.gov/pubmed/6857549>.
- A.W.F. Edwards. *Likelihood*. Cambridge Science Classics. Cambridge University Press, 1984. ISBN 9780521318716. URL <http://www.ams.org/mathscinet-getitem?mr=348869>.
- Charles L. Epstein and John Schotland. The bad truth about Laplace’s transform. *SIAM Review*, 50(3):504–520, 2008. ISSN 0036-1445. doi: 10.1137/060657273. URL <http://dx.doi.org/10.1137/060657273>.
- Jack N. Fenner. Cross-cultural estimation of the human generation interval for use in genetics-based population divergence studies. *American Journal of Physical Anthropology*, 128(2):415–423, 2005. ISSN 1096-8644. doi: 10.1002/ajpa.20188. URL <http://dx.doi.org/10.1002/ajpa.20188>.

- Ronald A Fisher. A fuller theory of ‘junctions’ in inbreeding. *Heredity*, 8(2):187–197, August 1954. ISSN 0018067X. URL <http://dx.doi.org/10.1038/hdy.1954.17>.
- S Giglio, K W Broman, N Matsumoto, V Calvari, G Gimelli, T Neumann, H Ohashi, L Voullaire, D Larizza, R Giorda, J L Weber, D H Ledbetter, and O Zuffardi. Olfactory receptor-gene clusters, genomic-inversion polymorphisms, and common chromosome rearrangements. *Am J Hum Genet*, 68(4):874–883, April 2001. doi: 10.1086/319506. URL <http://www.ncbi.nlm.nih.gov/pubmed/11231899>.
- Andrew Gillett. Ethnogenesis: A contested model of early medieval Europe. *History Compass*, 4(2):241–260, 2006. ISSN 1478-0542. doi: 10.1111/j.1478-0542.2006.00311.x. URL <http://dx.doi.org/10.1111/j.1478-0542.2006.00311.x>.
- S Gravel. Population genetics models of local ancestry. *Genetics*, 191(2):607–619, June 2012. doi: 10.1534/genetics.112.139808. URL <http://www.ncbi.nlm.nih.gov/pubmed/22491189?dopt=Abstract>.
- G.R. Grimmett and D.R. Stirzaker. *Probability and random processes*, volume 80. Oxford university press, 2001.
- Gusev, J K Lowe, M Stoffel, M J Daly, D Altshuler, J L Breslow, J M Friedman, and I Pe’er. Whole population, genome-wide mapping of hidden relatedness. *Genome Res*, 19(2):318–326, February 2009. doi: 10.1101/gr.081398.108. URL <http://www.ncbi.nlm.nih.gov/pmc/articles/PMC2652213>.
- Alexander Gusev, Pier Francesco Palamara, Gregory Aponte, Zhong Zhuang, Ariel Darvasi, Peter Gregersen, and Itsik Pe’er. The architecture of long-range haplotypes shared within and across populations. *Molecular Biology and Evolution*, 29(2):473–486, 2012. doi: 10.1093/molbev/msr133. URL <http://mbe.oxfordjournals.org/content/29/2/473.abstract>.
- Guy Halsall. The Barbarian invasions. In Paul Fouracre, editor, *The New Cambridge Medieval History*, number v. 1 in The New Cambridge Medieval History, chapter 2, pages 38–55. Cambridge University Press, 2005. ISBN 9780521362917. URL <http://books.google.com/books?id=JcmwuoTsK00C>.
- E.P. Hamp. The position of albanian. *Ancient Indo-European Dialects*, pages 97–121, 1966. URL <http://groznijat.tripod.com/balkan/ehamp.html>.
- B M Henn, L R Botigué, S Gravel, W Wang, A Brisbin, J K Byrnes, K Fadhlouli-Zid, P A Zalloua, A Moreno-Estrada, J Bertranpetit, C D Bustamante, and D Comas. Genomic ancestry of north africans supports back-to-africa migrations. *PLoS Genet*, 8(1), January 2012a. doi: 10.1371/journal.pgen.1002397. URL <http://www.ncbi.nlm.nih.gov/pubmed/22253600>.
- Brenna M. Henn, Lawrence Hon, J. Michael Macpherson, Nick Eriksson, Serge Saxonov, Itsik Pe’er, and Joanna L. Mountain. Cryptic distant relatives are common in both isolated and cosmopolitan genetic samples. *PLoS ONE*, 7(4):e34267, 04 2012b. doi: 10.1371/journal.pone.0034267.
- Arthur E. Hoerl and Robert W. Kennard. Ridge regression: Biased estimation for nonorthogonal problems. *Technometrics*, 12(1):pp. 55–67, 1970. ISSN 00401706. URL <http://www.jstor.org/stable/1267351>.
- R.R. Hudson. Gene genealogies and the coalescent process. *Oxford surveys in evolutionary biology*, 7(1):44, 1990.
- C. D. Huff, D. J. Witherspoon, T. S. Simonson, J. Xing, W. S. Watkins, Y. Zhang, T. M. Tuohy, D. W. Neklason, R. W. Burt, S. L. Guthery, S. R. Woodward, and L. B. Jorde. Maximum-likelihood estimation of recent shared ancestry (ERSA). *Genome Res.*, 21:768–774, May 2011. URL <http://www.ncbi.nlm.nih.gov/pubmed/21324875>.

- International HapMap Consortium, K A Frazer, D G Ballinger, D R Cox, D A Hinds, L L Stuve, R A Gibbs, J W Belmont, A Boudreau, P Hardenbol, S M Leal, S Pasternak, D A Wheeler, T D Willis, F Yu, H Yang, C Zeng, Y Gao, H Hu, W Hu, C Li, W Lin, S Liu, H Pan, X Tang, J Wang, W Wang, J Yu, B Zhang, Q Zhang, H Zhao, H Zhao, J Zhou, S B Gabriel, R Barry, B Blumenstiel, A Camargo, M Defelice, M Faggart, M Goyette, S Gupta, J Moore, H Nguyen, R C Onofrio, M Parkin, J Roy, E Stahl, E Winchester, L Ziaugra, D Altshuler, Y Shen, Z Yao, W Huang, X Chu, Y He, L Jin, Y Liu, Y Shen, W Sun, H Wang, Y Wang, Y Wang, X Xiong, L Xu, M M Wayne, S K Tsui, H Xue, J T Wong, L M Galver, J B Fan, K Gunderson, S S Murray, A R Oliphant, M S Chee, A Montpetit, F Chagnon, V Ferretti, M Leboeuf, J F Olivier, M S Phillips, S Roumy, C Sallée, A Verner, T J Hudson, P Y Kwok, D Cai, D C Koboldt, R D Miller, L Pawlikowska, P Taillon-Miller, M Xiao, L C Tsui, W Mak, Y Q Song, P K Tam, Y Nakamura, T Kawaguchi, T Kitamoto, T Morizono, A Nagashima, Y Ohnishi, A Sekine, T Tanaka, T Tsunoda, P Deloukas, C P Bird, M Delgado, E T Dermitzakis, R Gwilliam, S Hunt, J Morrison, D Powell, B E Stranger, P Whittaker, D R Bentley, M J Daly, P I de Bakker, J Barrett, Y R Chretien, J Maller, S McCarroll, N Patterson, I Pe'er, A Price, S Purcell, D J Richter, P Sabeti, R Saxena, S F Schaffner, P C Sham, P Varilly, D Altshuler, L D Stein, L Krishnan, A V Smith, M K Tello-Ruiz, G A Thorisson, A Chakravarti, P E Chen, D J Cutler, C S Kashuk, S Lin, G R Abecasis, W Guan, Y Li, H M Munro, Z S Qin, D J Thomas, G McVean, A Auton, L Bottolo, N Cardin, S Eyheramendy, C Freeman, J Marchini, S Myers, C Spencer, M Stephens, P Donnelly, L R Cardon, G Clarke, D M Evans, A P Morris, B S Weir, T Tsunoda, J C Mullikin, S T Sherry, M Feolo, A Skol, H Zhang, C Zeng, H Zhao, I Matsuda, Y Fukushima, D R Macer, E Suda, C N Rotimi, C A Adebamowo, I Ajayi, T Aniagwu, P A Marshall, C Nkwodimmah, C D Royal, M F Leppert, M Dixon, A Peiffer, R Qiu, A Kent, K Kato, N Niikawa, I F Adewole, B M Knoppers, M W Foster, E W Clayton, J Watkin, R A Gibbs, J W Belmont, D Muzny, L Nazareth, E Sodergren, G M Weinstock, D A Wheeler, I Yakub, S B Gabriel, R C Onofrio, D J Richter, L Ziaugra, B W Birren, M J Daly, D Altshuler, R K Wilson, L L Fulton, J Rogers, J Burton, N P Carter, C M Clee, M Griffiths, M C Jones, K McLay, R W Plumb, M T Ross, S K Sims, D L Willey, Z Chen, H Han, L Kang, M Godbout, J C Wallenburg, P L'Archevêque, G Bellemare, K Saeki, H Wang, D An, H Fu, Q Li, Z Wang, R Wang, A L Holden, L D Brooks, J E McEwen, M S Guyer, V O Wang, J L Peterson, M Shi, J Spiegel, L M Sung, L F Zacharia, F S Collins, K Kennedy, R Jamieson, and J Stewart. A second generation human haplotype map of over 3.1 million SNPs. *Nature*, 449(7164):851–861, October 2007. doi: 10.1038/nature06258. URL <http://www.ncbi.nlm.nih.gov/pubmed/17943122>.
- E Jakkula, K Rehnström, T Varilo, O P Pietiläinen, T Paunio, N L Pedersen, U deFaire, M R Järvelin, J Saharinen, N Freimer, S Ripatti, S Purcell, A Collins, M J Daly, A Palotie, and L Peltonen. The genome-wide patterns of variation expose significant substructure in a founder population. *Am J Hum Genet*, 83(6):787–794, December 2008. doi: 10.1016/j.ajhg.2008.11.005. URL <http://www.ncbi.nlm.nih.gov/pubmed/19061986>.
- A Keller, A Graefen, M Ball, M Matzas, V Boissguerin, F Maixner, P Leidinger, C Backes, R Khairat, M Forster, B Stade, A Franke, J Mayer, J Spangler, S McLaughlin, M Shah, C Lee, T T Harkins, A Sartori, A Moreno-Estrada, B Henn, M Sikora, O Semino, J Chikarini, S Rootsi, N M Myres, V M Cabrera, P A Underhill, C D Bustamante, E E Vigl, M Samadelli, G Cipollini, J Haas, H Katus, B D O'Connor, M R Carlson, B Meder, N Blin, E Meese, C M Pusch, and A Zink. New insights into the Tyrolean Iceman's origin and phenotype as inferred by whole-genome sequencing. *Nat Commun*, 3:698–698, 2012. doi: 10.1038/ncomms1701. URL <http://www.ncbi.nlm.nih.gov/pubmed/22426219>.
- J. F. C. Kingman. On the genealogy of large populations. *Journal of Applied Probability*, 19:27–43, 1982. ISSN 00219002. URL <http://www.jstor.org/stable/3213548>.
- Zbigniew Kobyliński. The Slavs. In Paul Fouracre, editor, *The New Cambridge Medieval History*, number v. 1 in The New Cambridge Medieval History, chapter 19, pages 524–544. Cambridge University Press, 2005. ISBN 9780521362917. URL <http://books.google.com/books?id=JcmwuoTsK00C>.
- O Lao, T T Lu, M Nothnagel, O Junge, S Freitag-Wolf, A Caliebe, M Balascakova, J Bertranpetit, L A Bindoff, D Comas, G Holmlund, A Kouvatsi, M Macek, I Mollet, W Parson, J Palo, R Ploski, A Sajan-

- tila, A Tagliabracci, U Gether, T Werge, F Rivadeneira, A Hofman, A G Uitterlinden, C Gieger, H E Wichmann, A R  ther, S Schreiber, C Becker, P N  rnberg, M R Nelson, M Krawczak, and M Kayser. Correlation between genetic and geographic structure in europe. *Curr Biol*, 18(16):1241–1248, August 2008. doi: 10.1016/j.cub.2008.07.049. URL <http://www.ncbi.nlm.nih.gov/pubmed/18691889>.
- Heng Li and Richard Durbin. Inference of human population history from individual whole-genome sequences. *Nature*, advance online publication:–, July 2011. ISSN 14764687. URL <http://dx.doi.org/10.1038/nature10231>.
- P Menozzi, A Piazza, and L Cavalli-Sforza. Synthetic maps of human gene frequencies in Europeans. *Science*, 201(4358):786–792, September 1978. URL <http://www.ncbi.nlm.nih.gov/pubmed/356262>.
- P. Moorjani, N. Patterson, J. N. Hirschhorn, A. Keinan, L. Hao, G. Atzmon, E. Burns, H. Ostrer, A. L. Price, and D. Reich. The history of African gene flow into Southern Europeans, Levantines, and Jews. *PLoS Genet.*, 7:e1001373, April 2011. URL <http://www.ncbi.nlm.nih.gov/pubmed/21533020>.
- M R Nelson, K Bryc, K S King, A Indap, A R Boyko, J Novembre, L P Briley, Y Maruyama, D M Waterworth, G Waeber, P Vollenweider, J R Oksenberg, S L Hauser, H A Stirnadel, J S Kooner, J C Chambers, B Jones, V Mooser, C D Bustamante, A D Roses, D K Burns, M G Ehm, and E H Lai. The Population Reference Sample, POPRES: a resource for population, disease, and pharmacological genetics research. *Am J Hum Genet*, 83(3):347–358, September 2008. doi: 10.1016/j.ajhg.2008.08.005. URL <http://www.ncbi.nlm.nih.gov/pmc/articles/PMC2556436>.
- Matthew R. Nelson, Daniel Wegmann, Margaret G. Ehm, Darren Kessner, Pamela St. Jean, Claudio Verzilli, Judong Shen, Zhengzheng Tang, Silviu-Alin Bacanu, Dana Fraser, Liling Warren, Jennifer Aponte, Matthew Zawistowski, Xiao Liu, Hao Zhang, Yong Zhang, Jun Li, Yun Li, Li Li, Peter Woolard, Simon Topp, Matthew D. Hall, Keith Nangle, Jun Wang, Gonalo Abecasis, Lon R. Cardon, Sebastian Zillner, John C. Whittaker, Stephanie L. Chisoe, John Novembre, and Vincent Mooser. An abundance of rare functional variants in 202 drug target genes sequenced in 14,002 people. *Science*, 2012. doi: 10.1126/science.1217876. URL <http://www.sciencemag.org/content/early/2012/05/16/science.1217876.abstract>.
- J Novembre and S Ramachandran. Perspectives on human population structure at the cusp of the sequencing era. *Annu Rev Genomics Hum Genet*, 12:245–274, September 2011. doi: 10.1146/annurev-genom-090810-183123. URL <http://www.ncbi.nlm.nih.gov/pubmed/21801023>.
- J Novembre, T Johnson, K Bryc, Z Kutalik, A R Boyko, A Auton, A Indap, K S King, S Bergmann, M R Nelson, M Stephens, and C D Bustamante. Genes mirror geography within Europe. *Nature*, 456(7218):98–101, November 2008. doi: 10.1038/nature07331. URL <http://www.ncbi.nlm.nih.gov/pubmed/18758442>.
- John Novembre and Matthew Stephens. Interpreting principal component analyses of spatial population genetic variation. *Nat Genet*, 40(5):646–649, May 2008. ISSN 1061-4036. URL <http://dx.doi.org/10.1038/ng.139>.
- C T O’Dushlaine, D Morris, V Moskvina, G Kirov, International Schizophrenia Consortium, M Gill, A Corvin, J F Wilson, and G L Cavalleri. Population structure and genome-wide patterns of variation in ireland and britain. *Eur J Hum Genet*, 18(11):1248–1254, November 2010. doi: 10.1038/ejhg.2010.87. URL <http://www.ncbi.nlm.nih.gov/pmc/articles/PMC2987482/>.
- Nick Patterson, Alkes L Price, and David Reich. Population structure and eigenanalysis. *PLoS Genet*, 2(12):e190, 12 2006. doi: 10.1371/journal.pgen.0020190. URL <http://dx.plos.org/10.1371%2Fjournal.pgen.0020190>.
- Y.P. Petrov and V.S. Sizikov. *Well-posed, ill-posed, and intermediate problems with applications*, volume 49. Walter de Gruyter, 2005.

- J E Pool and R Nielsen. Inference of historical changes in migration rate from the lengths of migrant tracts. *Genetics*, 181(2):711–719, February 2009. doi: 10.1534/genetics.108.098095. URL <http://www.ncbi.nlm.nih.gov/pubmed/19087958?dopt=Abstract>.
- J E Powell, P M Visscher, and M E Goddard. Reconciling the analysis of ibd and ibs in complex trait studies. *Nat Rev Genet*, 11(11):800–805, November 2010. doi: 10.1038/nrg2865. URL <http://www.ncbi.nlm.nih.gov/pubmed/20877324>.
- A L Price, A Helgason, S Palsson, H Stefansson, D St Clair, O A Andreassen, D Reich, A Kong, and K Stefansson. The impact of divergence time on the nature of population structure: an example from Iceland. *PLoS Genet*, 5(6), June 2009. doi: 10.1371/journal.pgen.1000505. URL <http://www.ncbi.nlm.nih.gov/pubmed/19503599>.
- S Purcell, B Neale, K Todd-Brown, L Thomas, M A Ferreira, D Bender, J Maller, P Sklar, P I de Bakker, M J Daly, and P C Sham. PLINK: a tool set for whole-genome association and population-based linkage analyses. *Am J Hum Genet*, 81(3):559–575, September 2007. doi: 10.1086/519795. URL <http://www.ncbi.nlm.nih.gov/pubmed/17701901>.
- R Development Core Team. *R: A Language and Environment for Statistical Computing*. R Foundation for Statistical Computing, Vienna, Austria, 2012. URL <http://www.R-project.org/>. ISBN 3-900051-07-0.
- Douglas L. T. Rohde, Steve Olson, and Joseph T. Chang. Modelling the recent common ancestry of all living humans. *Nature*, 431(7008):562–566, September 2004. ISSN 0028-0836. URL <http://dx.doi.org/10.1038/nature02842>.
- P Skoglund, H Malmström, M Raghavan, J Storå, P Hall, E Willerslev, M T Gilbert, A Götherström, and M Jakobsson. Origins and genetic legacy of Neolithic farmers and hunter-gatherers in Europe. *Science*, 336(6080):466–469, April 2012. doi: 10.1126/science.1216304. URL <http://www.ncbi.nlm.nih.gov/pubmed/22539720>.
- Soares, A Achilli, O Semino, W Davies, V Macaulay, H J Bandelt, A Torroni, and M B Richards. The archaeogenetics of europe. *Curr Biol*, 20(4):174–183, February 2010. doi: 10.1016/j.cub.2009.11.054. URL <http://www.ncbi.nlm.nih.gov/pubmed/20178764>.
- A. M. Stuart. Inverse problems: a Bayesian perspective. *Acta Numer.*, 19:451–559, 2010. ISSN 0962-4929. doi: 10.1017/S0962492910000061. URL <http://dx.doi.org/10.1017/S0962492910000061>.
- N Takahata. Allelic genealogy and human evolution. *Molecular Biology and Evolution*, 10(1):2–22, 1993. URL <http://mbe.oxfordjournals.org/content/10/1/2.abstract>.
- J A Tennessen, A W Bigham, T D O’Connor, W Fu, E E Kenny, S Gravel, S McGee, R Do, X Liu, G Jun, H M Kang, D Jordan, S M Leal, S Gabriel, M J Rieder, G Abecasis, D Altshuler, D A Nickerson, E Boerwinkle, S Sunyaev, C D Bustamante, M J Bamshad, J M Akey, Broad GO, Seattle GO, and on behalf of the NHLBI Exome Sequencing Project. Evolution and functional impact of rare coding variation from deep sequencing of human exomes. *Science*, May 2012. doi: 10.1126/science.1219240. URL <http://www.ncbi.nlm.nih.gov/pubmed/22604720>.
- Andrey N. Tikhonov and Vasiliy Y. Arsenin. *Solutions of ill-posed problems*. V. H. Winston & Sons, Washington, D.C.: John Wiley & Sons, New York, 1977. Translated from the Russian, Preface by translation editor Fritz John, Scripta Series in Mathematics.
- Berwin A. Turlach and Andreas Weingessel. *quadprog: Functions to solve Quadratic Programming Problems.*, 2011. URL <http://CRAN.R-project.org/package=quadprog>. R package version 1.5-4; S original by Berwin A. Turlach, R port by Andreas Weingessel.
- Chris Tyler-Smith and Yali Xue. A British approach to sampling. *Eur J Hum Genet*, 20(2):129–130, February 2012. ISSN 10184813. URL <http://dx.doi.org/10.1038/ejhg.2011.153>.

John Wakeley. *Coalescent Theory, an Introduction*. Roberts and Company, Greenwood Village, CO, 2005.
URL <http://www.coalescenttheory.com/>.

J. Wilkes. *The Illyrians*. The Peoples of Europe. John Wiley & Sons, 1996. ISBN 9780631198079.

Bruce Winney, Abdelhamid Boumertit, Tammy Day, Dan Davison, Chikodi Echeta, Irina Evseeva, Katarzyna Hutnik, Stephen Leslie, Kristin Nicodemus, Ellen C Royrvik, Susan Tonks, Xiaofeng Yang, James Cheshire, Paul Longley, Pablo Mateos, Alexandra Groom, Caroline Relton, D Tim Bishop, Kathryn Black, Emma Northwood, Louise Parkinson, Timothy M Frayling, Anna Steele, Julian R Sampson, Turi King, Ron Dixon, Derek Middleton, Barbara Jennings, Rory Bowden, Peter Donnelly, and Walter Bodmer. People of the British Isles: preliminary analysis of genotypes and surnames in a UK-control population. *Eur J Hum Genet*, pages –, August 2011. ISSN 14765438. URL <http://dx.doi.org/10.1038/ejhg.2011.127>.

Supplemental material

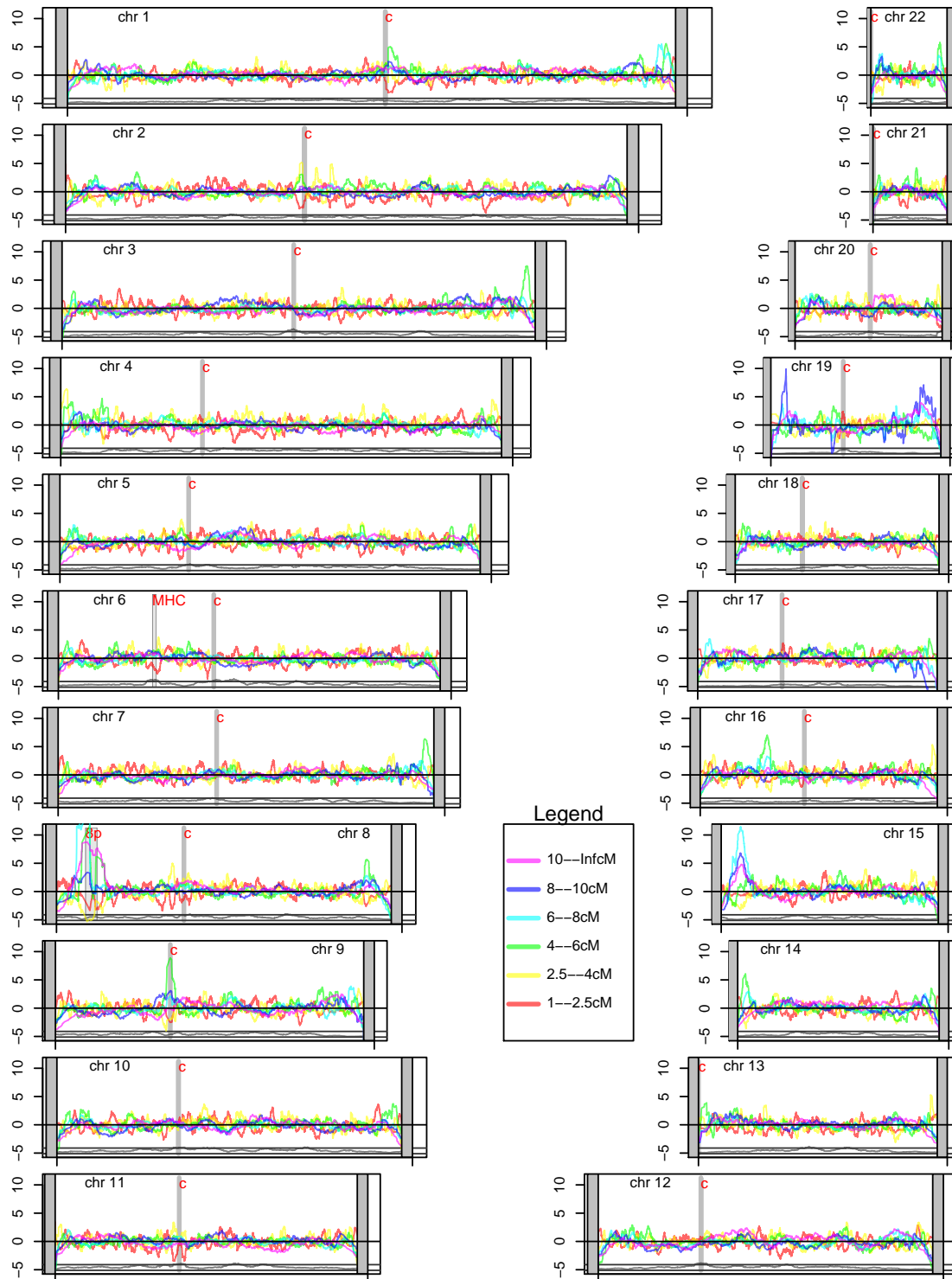


Figure S1: Normalized density of IBD blocks of different lengths, corrected for SNP density, across all autosomes (see section 4.4 for details). Marked with a grey bar and “c” are the centromeres; and marked with “8p” is a large, segregating inversion (Giglio et al., 2001). The grey curve along the bottom shows normalized SNP density.

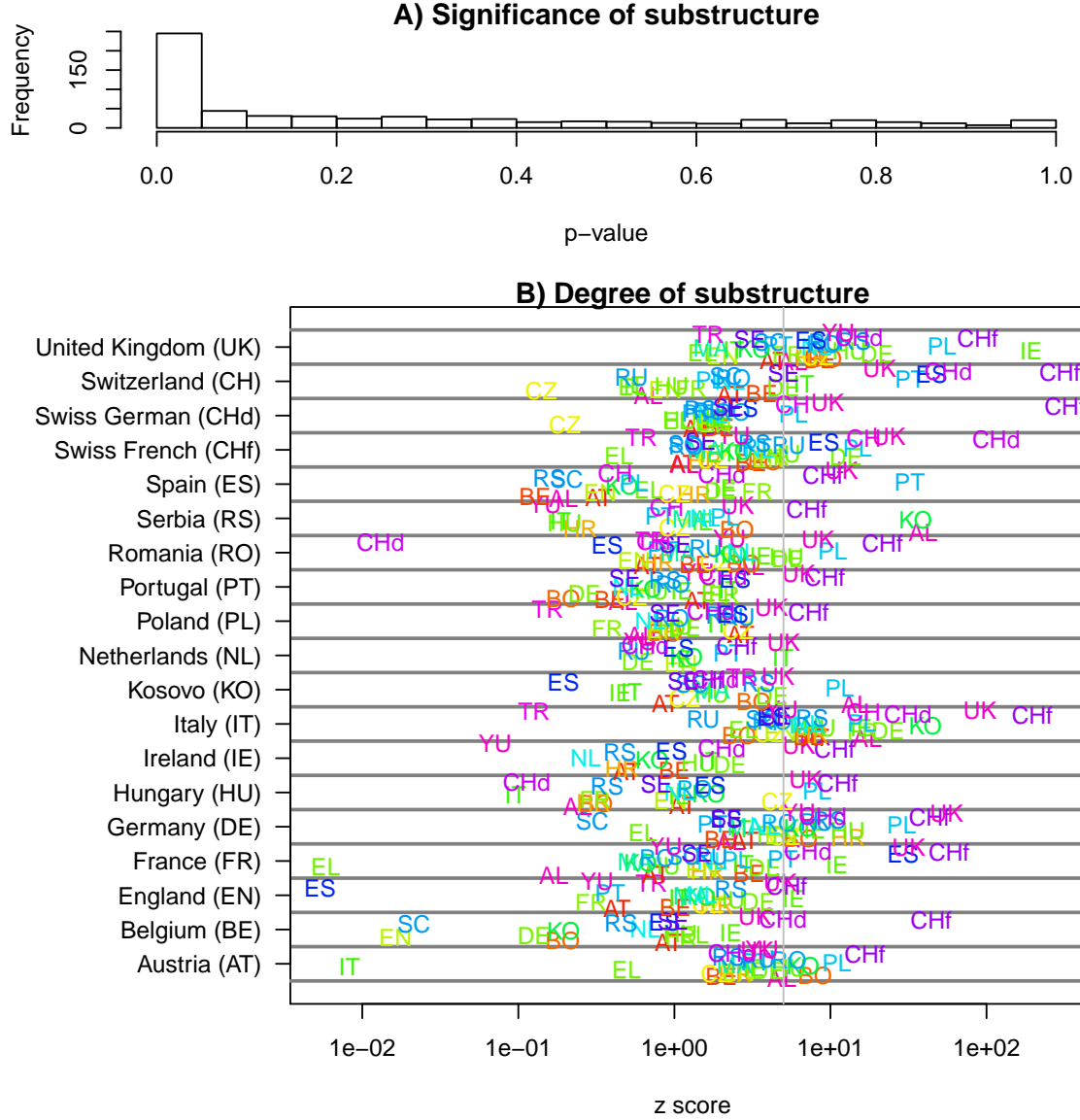


Figure S2: Two measures of overdispersal of block numbers across individuals (i.e. substructure): Suppose we have n individuals from population x , and N_{iy} is the number of IBD blocks of length at least 1cM that individual i shares with anyone from population y . Our statistic of substructure within x with respect to y is the variance of these numbers, $s_{xy} = \frac{1}{n-1} \left(\sum_i N_{iy}^2 - \frac{1}{n} \left(\sum_i N_{iy} \right)^2 \right)$. We obtained a “null” distribution for this statistic by randomly reassigning all blocks shared between x and y to an individual from x , and used this to evaluate the strength and the statistical significance of this substructure. **(A)** Histogram of the “ p -value”, of the proportion of 1000 replicates that showed a variance greater than or equal to the observed variance s_{xy} , for all pairs of populations x and y with at least 10 individuals in population y . **(B)** The “ z score”, which is observed value s_{xy} minus mean value divided by standard deviation, estimated using 1000 replicates. The population x is shown on the vertical axis, with text labels giving y , so for instance, Italians show much more substructure with most other populations than do Irish. Note that sample size still has a large effect – it is easier to see substructure with respect to the Swiss French ($x = \text{CHf}$) because the large number of Swiss French samples allows greater resolution. A vertical line is shown at $z = 5$. Only pairs of populations with at least 3 samples in country x and 10 samples in country y are shown. Because of the log scale, only pairs with a positive z score are shown, but no comparisons had $z < -2.5$, and only three had $z < -2$.

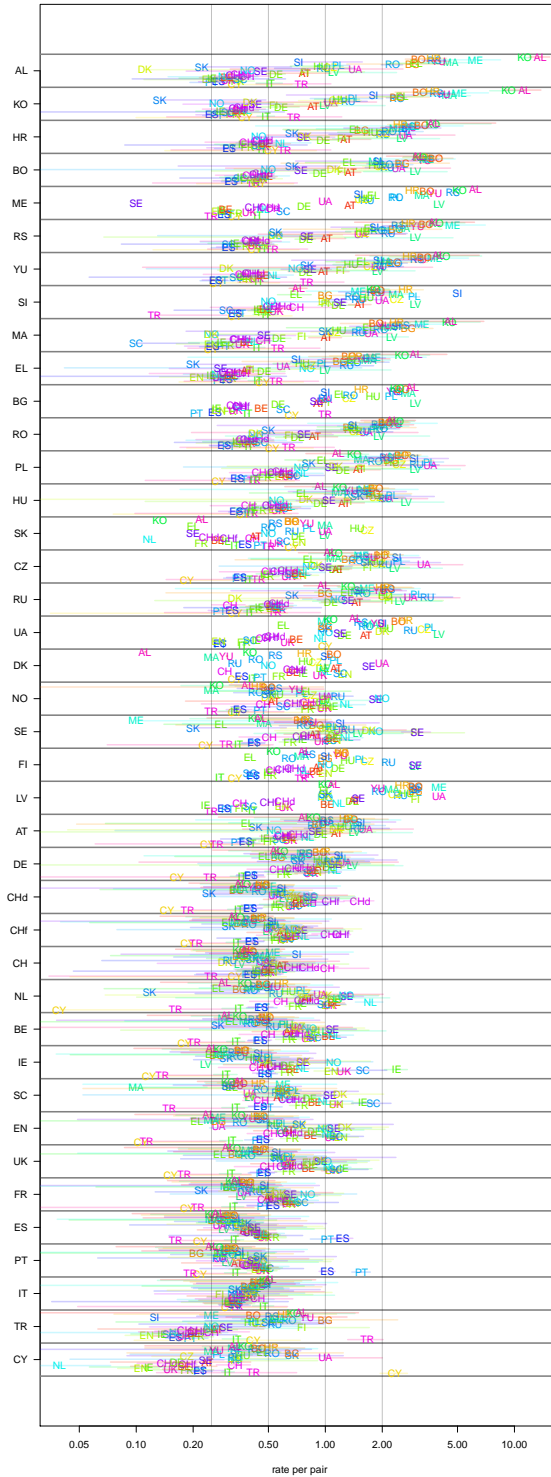


Figure S3: (A) Mean numbers of IBD blocks of length at least 1cM per pair of individuals, shown as a modified Cleveland dotchart, with ± 2 standard deviations shown as horizontal lines. For instance, on the bottom row we see that someone from the UK shares on average about one IBD block with someone else from the UK and slightly less than 0.2 blocks with someone from Turkey. Note that in most cases, the distribution of block numbers is fairly concentrated, and that nearby populations show quite similar patterns.

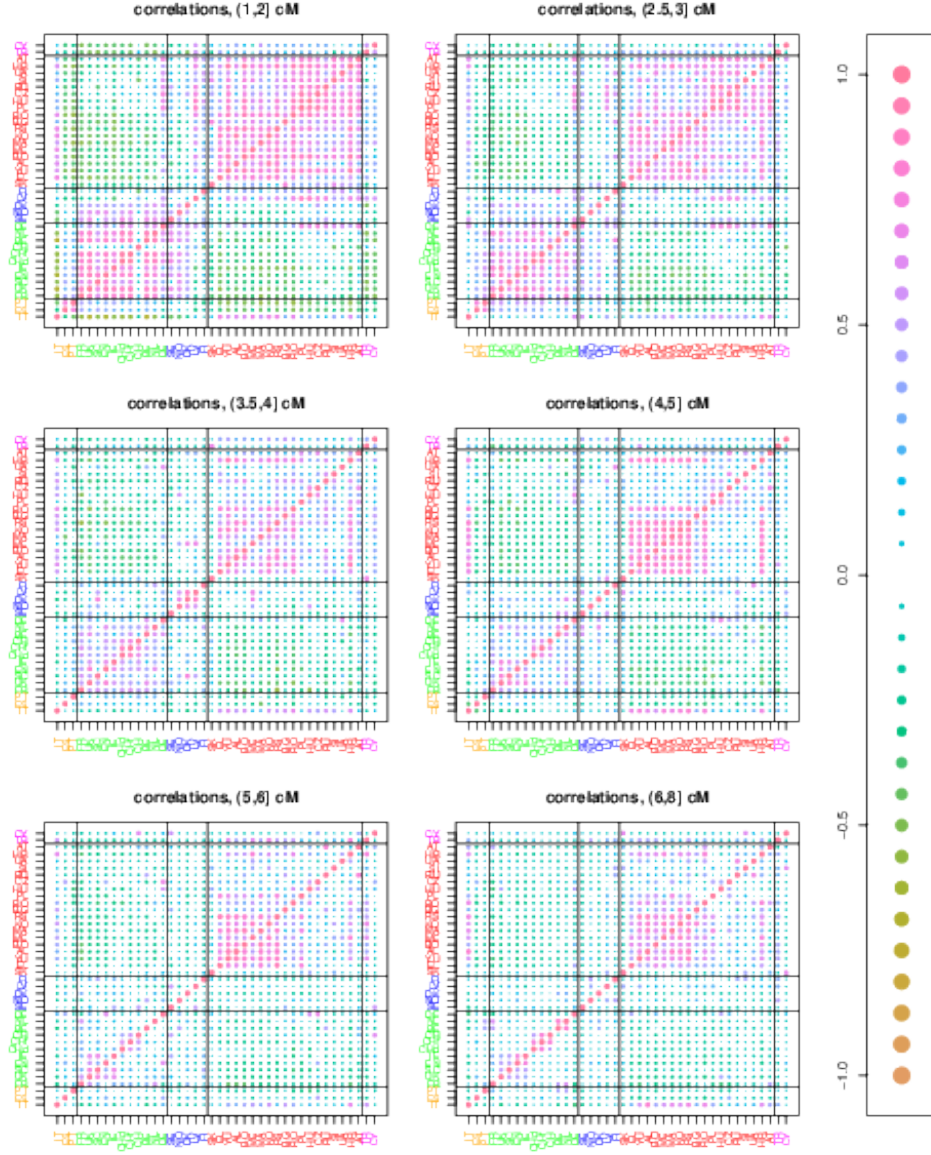


Figure S4: Correlations in IBD rates, for six different length windows (omitted length windows are similar). If there are n populations, $I(x, y)$ is the mean number of blocks in the given length range shared by a pair from populations x and y , and $\bar{I}(x) = (1/(n-1)) \sum_{z \neq x} I(x, z)$, shown is $(1/(n-2)) \sum_{z \notin \{x, y\}} (I(x, z) - \bar{I}(x))(I(y, z) - \bar{I}(y))$.

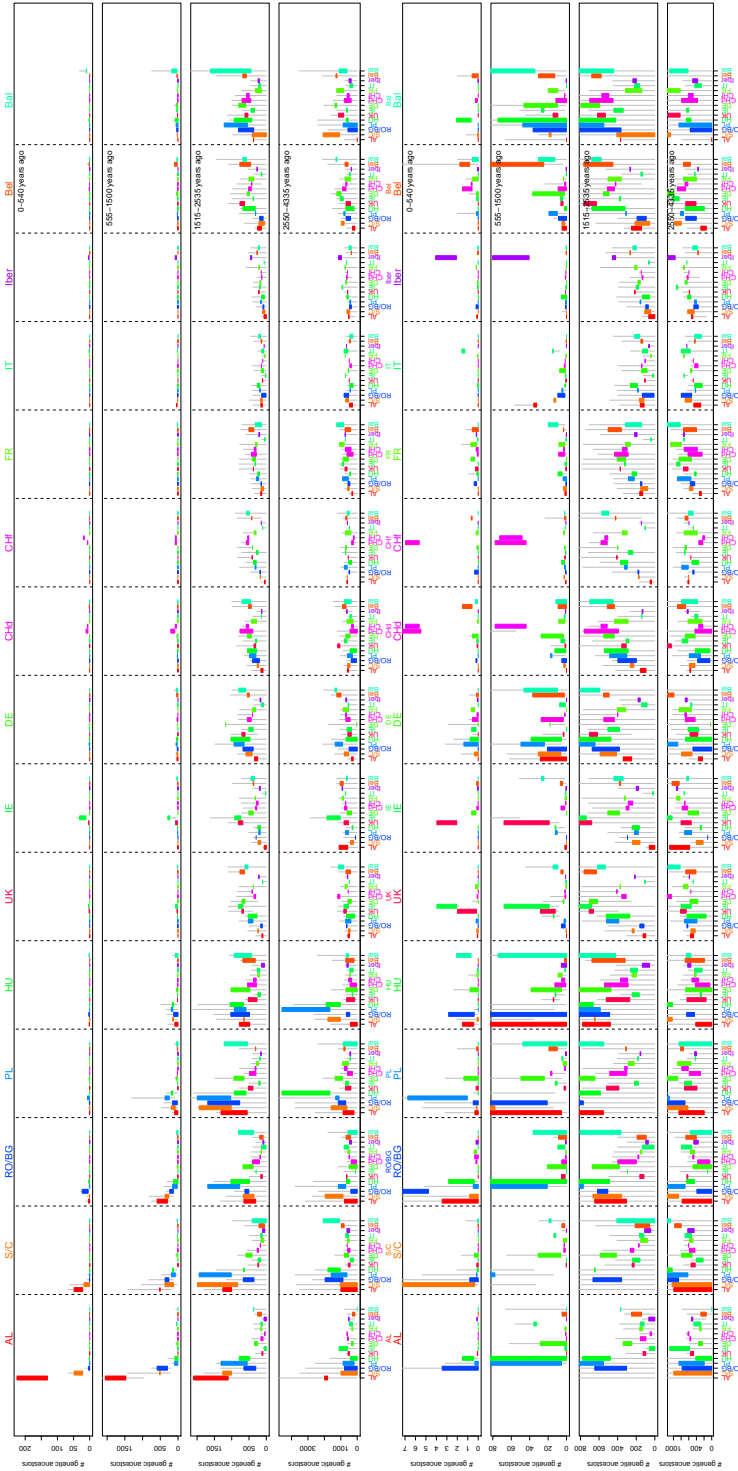


Figure S5: Estimated total numbers of genetic common ancestors shared by various pairs of populations, in roughly the time periods 0–500ya, 500–1500ya, 1500–2500ya, and 2500–4300ya. The two sets of figures are identical, except with different limits on the vertical axis – this is done because of the large differences in scale between different populations. The population groupings are: “AL”, Albanian speakers (Albania and Kosovo); “S-C”, Serbo-Croatian speakers in Bosnia, Croatia, Serbia, Montenegro, and Yugoslavia; “R-B”, Romania and Bulgaria; “UK”, United Kingdom, England, Scotland, Wales; “Iber”, Spain and Portugal; “Bel”, Belgium and the Netherlands; “Bal”, Latvia, Finland, Sweden, Norway, and Denmark; and denotes a single population with the same abbreviations as in table 1 otherwise.

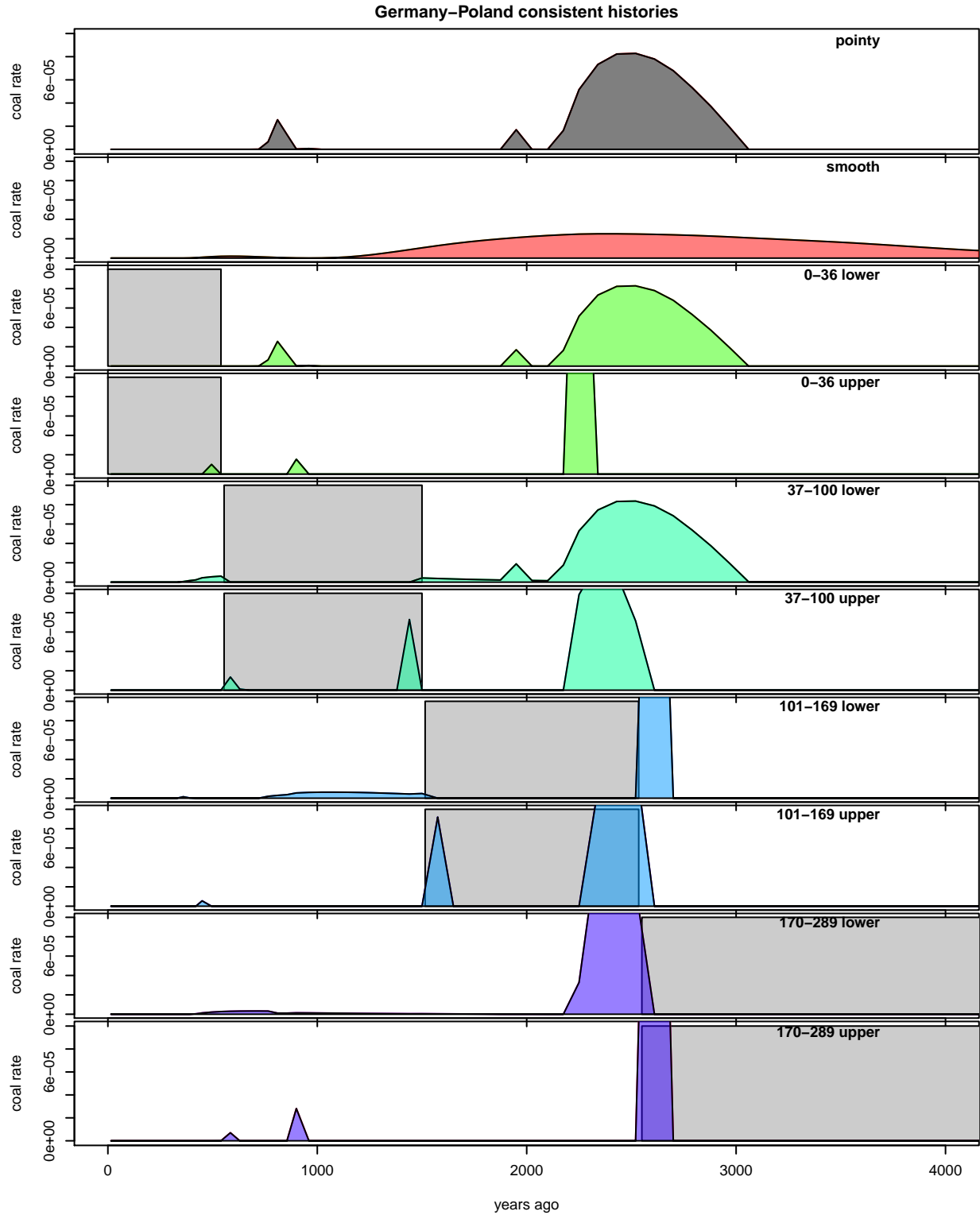


Figure S6: An example of the set of consistent histories (numbers of genetic common ancestors back through time) used to find upper and lower bounds in figures S5 and 5. The example shown is Poland–Germany; “pointy” is the maximum likelihood history; “smooth” is the smoothest consistent history; and the remaining plots show the histories giving lower and upper bounds for the referenced time intervals (in numbers of generations). In each case, the segment of time on which we are looking for a bound is shaded.

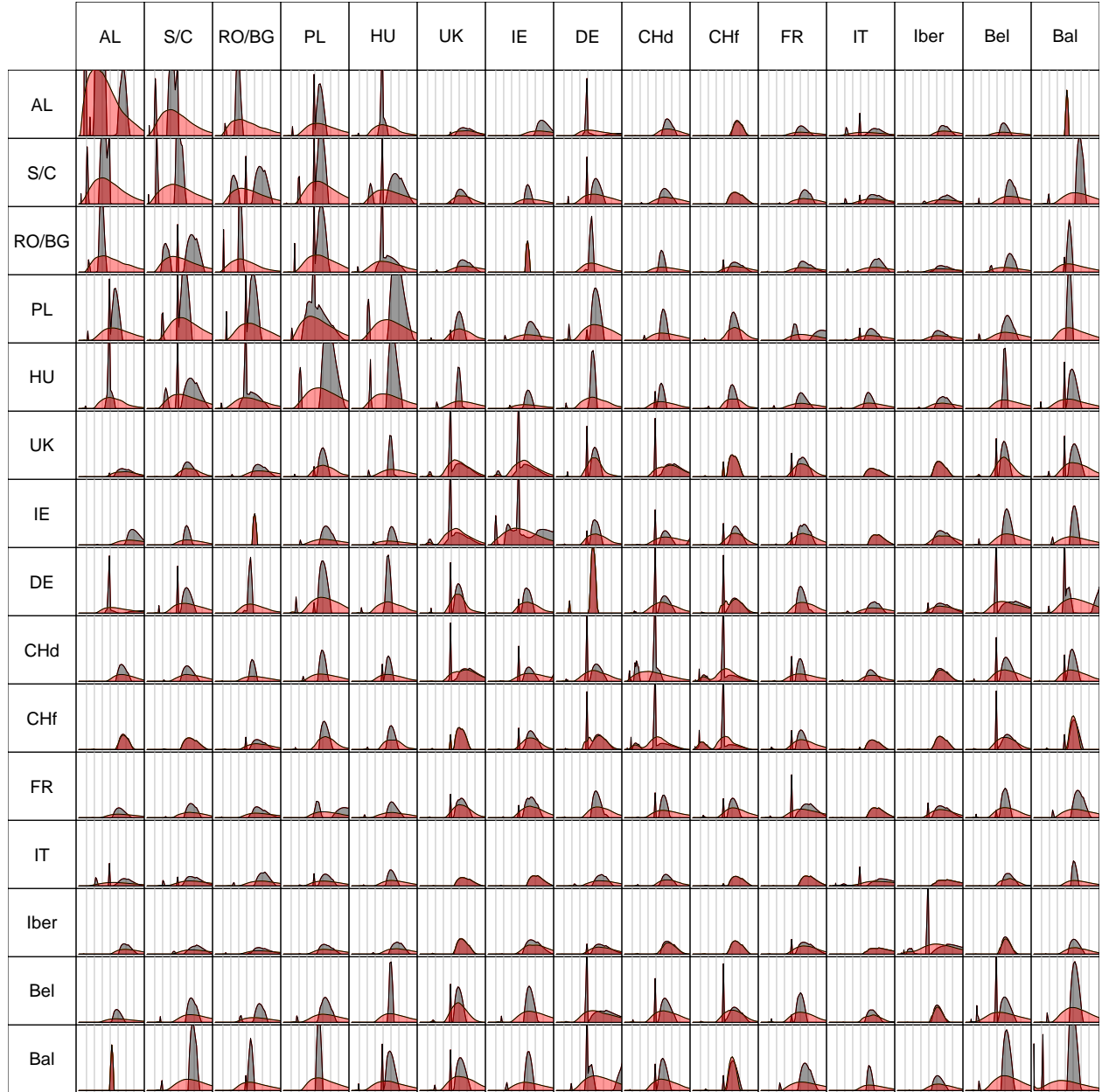


Figure S7: The maximum likelihood history (grey) and smoothest consistent history (red) for all pairs of population groupings of figure S5 (including those of figure 5). Each panel is analogous to a panel of figure 4; time scale is given by vertical grey lines every 500 years. For these plots on a larger scale see supplemental figure S8.

COUNTRY_SELF	COUNTRY_GFOLX	PRIMARY_LANGUAGE	Population	<i>n</i>
Albania	Albania	Albanian	Albania	3
Yugoslavia	Serbia	Albanian	Albania	1
Yugoslavia	Yugoslavia	Albanian	Albania	5
Austria		German	Austria	3
Austria	Austria	German	Austria	10
Spain	Austria	German	Austria	1
Belgium	Belgium	Dutch	Belgium	4
Belgium	Belgium	Flemish	Belgium	3
Belgium	Belgium	French	Belgium	28
Germany	Belgium	French	Belgium	1
Switzerland	Belgium	French	Belgium	1
Bosnia	Bosnia	Bosnian	Bosnia	4
Bosnia	Bosnia	Serbian	Bosnia	1
Bosnia	Bosnia	Serbo-Croatian	Bosnia	4
Bulgaria	Bulgaria	Bulgarian	Bulgaria	1
Croatia		Croatian	Croatia	1
Croatia	Croatia	Croatian	Croatia	6
Yugoslavia	Yugoslavia	Croatian	Croatia	1
Croatia	Croatia	Serbo-Croatian	Croatia	1
Cyprus		English	Cyprus	1
Cyprus		Greek	Cyprus	1
Cyprus	Cyprus	Greek	Cyprus	1
Czech Republic	Czech Republic	Czech	Czech Republic	9
Denmark		Danish	Denmark	1
England	England	English	England	18
Turkey	England	English	England	1
United Kingdom	England	English	England	3
Finland	Finland	Finnish	Finland	1
France		French	France	2
France	France	French	France	82
Germany	France	French	France	1
Switzerland	France	French	France	1
Germany			Germany	1
Germany		English	Germany	2
Germany	Germany	French	Germany	1
Germany		German	Germany	1
Germany	Germany	German	Germany	63
Switzerland	Germany	German	Germany	1
Hungary	Germany	Hungarian	Germany	1
Germany	Germany	Polish	Germany	1
Switzerland	Greece	French	Greece	1
Greece	Greece	Greek	Greece	4

(continued on next page)

Table S1: The composition of our populations. “COUNTRY_SELF” is the reported country of origin; “COUNTRY_GFOLX” is the country of origin of all reported grandparents (individuals with reported grandparents from different countries were removed); “PRIMARY_LANGUAGE” is the reported primary language; “Population” is our population label; and *n* gives the number of individuals falling in this category.

COUNTRY_SELF	COUNTRY_GFOLX	PRIMARY_LANGUAGE	Population	<i>n</i>
Hungary	Hungary	French	Hungary	1
Hungary	Hungary	Hungarian	Hungary	17
Hungary	Hungary	Russian	Hungary	1
Ireland			Ireland	19
Ireland		English	Ireland	38
England	Ireland	English	Ireland	1
Ireland	Ireland	English	Ireland	1
Ireland	Ireland	French	Ireland	1
Italy			Italy	1
France	Italy	French	Italy	1
Italy	Italy	French	Italy	8
Switzerland	Italy	French	Italy	9
Italy	Italy	German	Italy	1
Italy		Italian	Italy	3
France	Italy	Italian	Italy	1
Italy	Italy	Italian	Italy	170
Romania	Italy	Italian	Italy	1
Sweden	Italy	Italian	Italy	1
Switzerland	Italy	Italian	Italy	17
Kosovo			Kosovo	1
Yugoslavia	Kosovo	Albanian	Kosovo	10
Yugoslavia	Kosovo	Kosovan	Kosovo	2
Yugoslavia	Kosovo	Serbo-Croatian	Kosovo	2
Latvia	Latvia	Latvian	Latvia	1
Macedonia	Macedonia	Macedonian	Macedonia	4
Yugoslavia	Montenegro	Serbian	Montenegro	1
Netherlands	Netherlands	Dutch	Netherlands	15
Holland		English	Netherlands	1
Netherlands	Netherlands	French	Netherlands	1
Norway	Norway	Norwegian	Norway	2
France	Poland	French	Poland	1
Poland		Polish	Poland	4
France	Poland	Polish	Poland	2
Poland	Poland	Polish	Poland	15
France	Portugal	Portuguese	Portugal	1
Portugal	Portugal	Portuguese	Portugal	114
Romania	Romania	Romanian	Romania	14
Romania	Russia	Romanian	Russia	1
Russia	Russia	Russian	Russia	5
Scotland		English	Scotland	3
Scotland	Scotland	English	Scotland	2
Yugoslavia	Serbia	Hungarian	Serbia	1
Serbia	Serbia	Serbian	Serbia	1
Yugoslavia	Serbia	Serbian	Serbia	4
Yugoslavia	Yugoslavia	Serbian	Serbia	2
Croatia	Serbia	Serbo-Croatian	Serbia	1
Yugoslavia	Serbia	Serbo-Croatian	Serbia	2
(continued on next page)				

Table S2: Continuation of table S1.

COUNTRY_SELF	COUNTRY_GFOLX	PRIMARY_LANGUAGE	Population	<i>n</i>
Slovakia	Slovakia	Slovakian	Slovakia	1
Italy	Slovenia	Slovene	Slovenia	1
Slovenia	Slovenia	Slovene	Slovenia	1
Spain	Spain	Columbia	Spain	2
Switzerland	Spain	Columbia	Spain	2
Spain	Spain	French	Spain	5
Switzerland	Spain	French	Spain	2
Spain	Spain	Galician	Spain	2
Spain		Spanish	Spain	4
Spain	Spain	Spanish	Spain	106
Switzerland	Spain	Spanish	Spain	7
Sweden			Sweden	1
Sweden	Sweden	Swedish	Sweden	9
Switzerland		French	Swiss French	1
Belgium	Switzerland	French	Swiss French	1
Czech Republic	Switzerland	French	Swiss French	1
France	Switzerland	French	Swiss French	7
Poland	Switzerland	French	Swiss French	1
Portugal	Switzerland	French	Swiss French	1
Spain	Switzerland	French	Swiss French	1
Switzerland	Switzerland	French	Swiss French	826
Switzerland	Switzerland	German	Swiss German	103
Italy	Switzerland	Italian	Switzerland	2
Switzerland	Switzerland	Italian	Switzerland	12
Switzerland	Switzerland	Patois	Switzerland	1
Switzerland	Switzerland	Romansch	Switzerland	1
Spain	Switzerland	Spanish	Switzerland	1
Turkey	Turkey	Turkish	Turkey	4
Ukraine	Ukraine	Ukrainian	Ukraine	1
United Kingdom			United Kingdom	87
United Kingdom		English	United Kingdom	270
United Kingdom	United Kingdom	English	United Kingdom	1
Yugoslavia			Yugoslavia	1
Yugoslavia	Yugoslavia	French	Yugoslavia	1
Yugoslavia	Yugoslavia	Romanian	Yugoslavia	1
Yugoslavia	Yugoslavia	Serbo-Croatian	Yugoslavia	3
Yugoslavia	Yugoslavia	Yugoslavian	Yugoslavia	4

Table S3: Continuation of table S2.

<http://www.eve.ucdavis.edu/~plralph/ibd/boxplotted-inversions.pdf>

Figure S8: All inversions shown in S7, one per page (225 pages total). There is one page per pair of comparisons used in figure 5. On each page, there is one large plot, showing 10 distinct consistent histories (numbers of genetic ancestors back through time), and below are 10 histograms of IBD block length, one for each consistent history, showing both the observed distribution and the partitioning of blocks into age categories predicted by that history. The names of the two groupings are shown in the upper right: “pointy” is the unconstrained maximum likelihood solution; “smooth” is the smoothest consistent history; “ $a-b$ lower” is the history used to find the lower bound for the time period $a-b$ generations ago in figure 5; and “ $a-b$ upper” is the history used to find the corresponding upper bound. Each of these are described in more detail in the Methods.